Complete Relative Stereochemistry of Maitotoxin

Wanjun Zheng, John A. DeMattei, Jiang-Ping Wu, James J.-W. Duan, Laura R. Cook, Hitoshi Oinuma, and Yoshito Kishi*

Contribution from the Department of Chemistry, Harvard University, Cambridge, Massachusetts 02138

Received April 15, 1996[⊗]

Abstract: By addressing the relative stereochemistry of the four acyclic portions via organic synthesis, the complete relative stereochemistry of maitotoxin (MTX) has been established as **1B**. The relative stereochemistry of the C.1−C.15 portion was elucidated via a two-phase approach: (1) the synthesis of the eight diastereomers possible for model **C**, representing the C.1−C.11 portion, and the eight diastereomers possible for model **D**, representing the C.11−C.15 portion, and the comparison of their proton and carbon NMR characteristics with those of MTX, concluding that **9** and **35** represent the relative stereochemistry of the corresponding portions of MTX; (2) the synthesis of the two remote diastereomers **51** and **52**, and comparison of their proton and carbon NMR characteristics with those of MTX, concluding that **51** represents the relative stereochemistry of the C.1−C.15 portion of MTX. The relative stereochemistry of the C.35−C.39, C.63−C.68, and C.134−C.142 acyclic portions was established via (1) the synthesis of the 8, 8, and 16 diastereomers possible for models **E**, **F**, and **G**, respectively, and (2) the comparison of their proton and carbon NMR characteristics with those of MTX, concluding that **81**, **117**, and **187**, respectively, represent the relative stereochemistry of the corresponding portions of MTX. Some biogenetic considerations have been given to speculate on the absolute configuration of MTX. The vicinal proton coupling constants observed for models **51**, **81**, **117**, and **187** were used to elucidate their preferred solution conformation. Assembling the preferred solution conformations found for the four acyclic portions allows one to suggest that the approximate global conformation of MTX is represented by the shape of a hook, with the C.35−C.39 portion being its curvature. MTX appears to be conformationally relatively rigid, except for conformational flexibility around the C.7−C.9 and C.12−C.14 portions. On the basis of the experimental results gained in the current work, coupled with those in the AAL-toxin/fumonisin area, it has been pointed out that the structural properties of **51**, **81**, **117**, **187** and their diastereomers are inherent to the specific stereochemical arrangement of the small substituents on the carbon backbone and are independent from the rest of the molecule. Thus, it has been suggested that each of these diastereomers has the capacity to install a unique structural characteristic through a specific stereochemical arrangement of substituents on the carbon backbone, and that fatty acids and related classes of compounds may be able to carry specific information and serve as functional materials in addition to structural materials.

I. Introduction

Ciguatera is a type of poisoning induced by ingestion of coral reef fish, which annually affects an estimated 20 000 people worldwide.[1] The toxification mechanism of these species was not known until 1976, when Yasumoto and co-workers showed that the epiphytic dinoflagellate *Gambierdiscus toxicus* is the causative organism whose toxins are transferred to the coral biota through the food chain, ultimately residing in carnivorous fish.[2] Several extraordinarily complex natural products, including ciguatoxin, which was isolated by Scheuer in 1967[3] and the structure of which was elucidated by Yasumoto in 1989,[4] were identified as the toxic principles of *G. toxicus*.[1a] Among these, maitotoxin (MTX; **1A**, Figure 1) is unique in terms of its molecular size and structural complexity as well as its extremely potent bioactivity. MTX is known to trigger a wide variety of biological events; most notably, it has been shown to act on the voltage-sensitive Ca^{2+} channels.[5]

Yasumoto has played the seminal role in the advancement of the chemistry of MTX, including its isolation and structure elucidation.[6] The gross structure of MTX was elucidated in 1993. The relative stereochemistry of the fused rings as well as the directly connected ether rings was reported in 1994. However, the relative stereochemistry of the chiral centers embedded in the four acyclic portions, i.e., at the C.1−C.15, C.35−C.39, C.63−C.68, and C.134−C.142 portions,[7] remained unknown. In this paper, we present our efforts to establish the relative stereochemistry of these four acyclic portions, and consequently the complete relative stereochemistry of MTX, via organic synthesis. On the basis of the vicinal proton coupling constants observed for the models of these four acyclic portions, we also suggest the preferred solution conformation of MTX.[8−10]

[⊗] Abstract published in *Advance ACS Abstracts,* August 1, 1996.

(1) For recent reviews, see: (a) Yasumoto, T.; Murata, M. *Chem. Rev.* **1993**, *93*, 1897−1909. (b) Faulkner, D. J. *Nat. Prod. Rep.* **1995**, *12*, 223−269. (c) Strichartz, G.; Castle, N. *Pharmacology of marine toxins. Effects on membrane channels*; ACS Symposium Series 418; American Chemical Society: Washington, DC, 1990; pp 2−20.

(2) Yasumoto, T.; Bagnis, R.; Vernoux, J. P. *Bull. Jpn. Soc. Sci. Fish.* **1976**, *42*, 359−365.

(3) (a) Scheuer, P. J.; Takahashi, W.; Tsutsumi, J.; Yoshida, T. *Science* **1967**, *155*, 1267−1268. (b) Nukina, M.; Koyanagi, L. M.; Scheuer, P. J. *Toxicon* **1984**, *22*, 169−176.

(4) Murata, M.; Legrand, A. M.; Ishibashi, Y.; Yasumoto, T. *J. Am. Chem. Soc.* **1989**, *111*, 8929−8931.

(5) (a) Takahashi, M.; Ohizumi, Y.; Yasumoto, T. *J. Biol. Chem.* **1982**, *257*, 7287−7289. (b) Kobayashi, M.; Ochi, R.; Ohizumi, Y. *Br. J. Pharmacol.* **1987**, *92*, 665−671. (c) Soergel, D. G.; Yasumoto, T.; Daly, J. W.; Gusovsky, F. *Mol. Pharmacol.* **1992**, *41*, 487−493.

(6) (a) Murata, M.; Iwashita, T.; Yokoyama, A.; Sasaki, M.; Yasumoto, T. *J. Am. Chem. Soc.* **1992**, *114*, 6594−6596. (b) Murata, M.; Naoki, H.; Iwashita, T.; Matsunaga, S.; Sasaki, M.; Yokoyama, A.; Yasumoto, T. *J. Am. Chem. Soc.* **1993**, *115*, 2060−2062. (c) Murata, M.; Naoki, H.; Matsunaga, S.; Satake, M.; Yasumoto, T. *J. Am. Chem. Soc.* **1994**, *116*, 7098−7107. (d) Satake, M.; Ishida, S.; Yasumoto, T. *J. Am. Chem. Soc.* **1995**, *117*, 7019−7020.

(7) The numbering used throughout this paper represents the position of the corresponding carbon atom in MTX.

S0002-7863(96)01230-9 CCC: $12.00

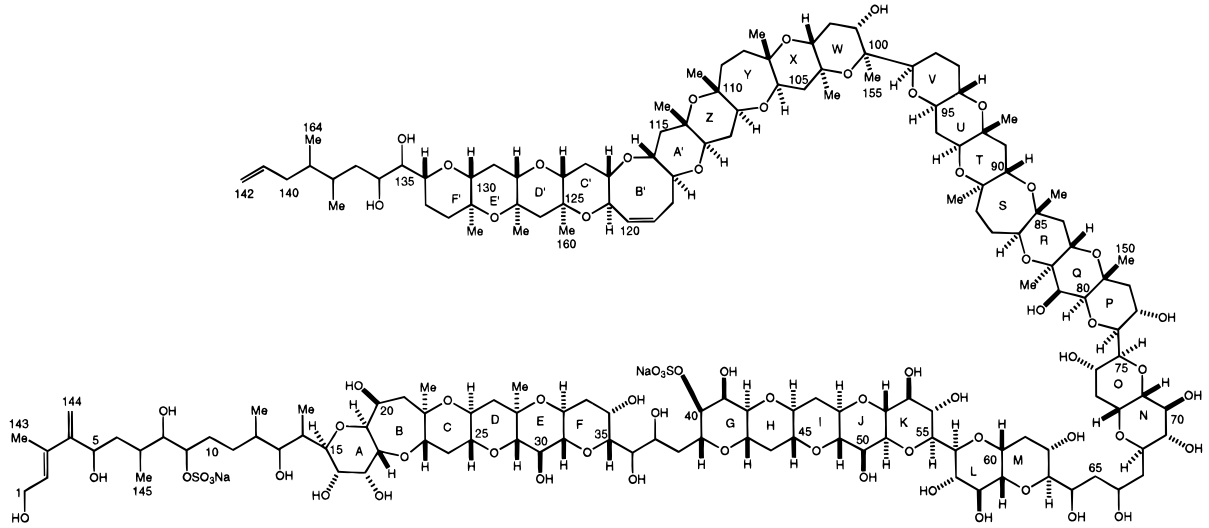

Figure 1. 1A: Maitotoxin.

II. Relative Stereochemistry

1. C.1−C.15 Acyclic Portion. This portion of MTX contains seven unassigned chiral centers on the acyclic backbone. In order to establish the complete relative stereochemistry of MTX, the configuration of these chiral centers relative to the C.15 position must also be addressed. Therefore, 128 possible diastereomers exist to represent the relative stereochemistry of this portion of MTX. A new concept was recently advanced to address this type of problem, and its validity and usefulness were demonstrated by the stereochemical assignment of the AAL-toxin/fumonisin family of natural products.[11]

This concept was first illustrated using AAL toxin T_A. The backbone of AAL toxin T_A had seven unknown asymmetric centers, and therefore there were 64 possible enantiomeric pairs of diastereomers to represent its stereochemistry. Its stereochemistry could be established via organic synthesis; namely, all of the possible diastereomers could be synthesized and compared with the aminopentol backbone derived from the natural product. However, there were two concerns about this standard approach. First, the synthesis of 64 possible enantiomeric pairs of diastereomers represented a substantial effort. Second, and more critically, even if all of the possible diastereomers were prepared, there was no assurance that all of them could be differentiated by currently available spectroscopic and/or chromatographic techniques.

The new approach consisted of three phases. The aminopentol backbone derived from AAL toxin T_A was composed of two distinct halves with the asymmetric centers separated by five methylene units (Scheme 1). This separation was assumed to be great enough for each half to have chemical properties

Scheme 1

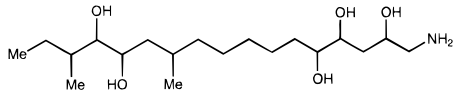

AAL Toxin T_A Backbone

Phase I

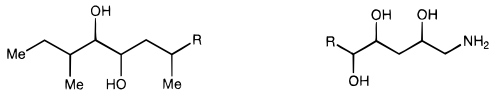

A : R = $CH_2CH_2CH{=}CMe_2$ **B** : R = $(CH_2)_6Me$

Phase II

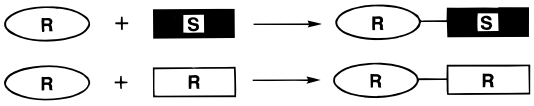

Phase III

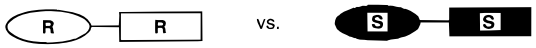

independent from its opposite half. Thus, models **A** and **B** should represent the relative stereochemical characteristics of the left and right halves of the AAL toxin T_A backbone, respectively. With this assumption, the first phase of this approach involved (1) the choice of models **A** and **B** properly representing the structural characteristics of the left and right halves of AAL toxin T_A, respectively; (2) the synthesis of all the diastereomers possible for **A** and **B**; and (3) the determination of which stereoisomers of **A** and **B** represent the left and right halves of the AAL toxin T_A aminopentol backbone, respectively. There were eight diastereomers possible for the left half and four diastereomers possible for the right half. Therefore, this operation required the synthesis of only 12 diastereomers instead of 64 and would allow us to determine the relative stereochemistry of the left and right halves of the aminopentol backbone of AAL toxin T_A.

The second phase was to determine the relative stereochemistry between the left and right halves of the AAL toxin T_A backbone. The left half is represented by an oval, and since only the relative stereochemistry of the left half would be known

(8) The complete relative stereochemistry of MTX was given as a part of the presentation at the Glaxo symposium (November 1995), the Prelog lecture (November 1995), and the 211th National Meeting of the American Chemical Society (March 1996) by one (Y.K.) of us.

(9) Since we began our work, Tachibana and co-workers reported the relative stereochemistry of the C.35−C.39 and C.63−C.68 portions of MTX: (a) Sasaki, M.; Matsumori, N.; Murata, M.; Tachibana, K.; Yasumoto, T. *Tetrahedron Lett.* **1995**, *36*, 9011−9014. (b) Sasaki, M.; Nonomura, T.; Murata, M.; Tachibana, K. *Tetrahedron Lett.* **1995**, *36*, 9007−9010.

(10) We thank Professor Murata for a preprint, discussing the C.5−C.9 relative stereochemistry assignment by long-range carbon−proton coupling constants: Matsumori, N.; Nonomura, T.; Sasaki, M.; Murata, M.; Tachibana, K.; Satake, M.; Yasumoto, T. *Tetrahedron Lett.* **1996**, *37*, 1269−1272.

(11) (a) Boyle, C. D.; Harmange, J.-C.; Kishi, Y. *J. Am. Chem. Soc.* **1994**, *116*, 4995−4996. (b) Harmange, J.-C.; Boyle, C. D.; Kishi, Y. *Tetrahedron Lett.* **1994**, *35*, 6819−6822. (c) Boyle, C. D.; Kishi, Y. *Tetrahedron Lett.* **1995**, *36*, 5695−5698 and references cited therein.

at this stage, it could exist in either an *R* or *S* configuration. The same holds true for the right half, which is depicted as a rectangle. Coupling of the *R* left half with the *S* right half would provide an *R*−*S* aminopentol backbone. Likewise, coupling of the *R* left half with the *R* right half would yield an *R*−*R* aminopentol backbone. In the case of diastereomers bearing chiral centers in close proximity, the pair could be distinguished from each other. However, as the diastereomers in question had chiral centers at remote positions (we refer to such cases as *remote diastereomers*), the degree of chemical communication between the two remote moieties should be negligibly small, if any exists. Indeed, the proposed first phase of this approach relied on this very assumption. We planned to apply the concept of molecular recognition to distinguish these remote diastereomers from each other. Interactions of these diastereomers with an achiral foreign molecule might differ significantly enough to be detected by currently available spectroscopic and/or chromatographic techniques.

The final phase of this approach was to distinguish the enantiomers of the AAL toxin T_A aminopentol backbone, i.e., *R*−*S* vs *S*−*R* or *R*−*R* vs *S*−*S*. This problem could be solved by several methods, including the possibility of using a chiral, instead of achiral, foreign molecule for molecular recognition. The validity and usefulness of this approach was demonstrated first for determination of the relative and absolute stereochemistry of the aminopentol backbone of AAL toxin T_A and then for the aminotetrol backbone of fumonisin B_2.[11]

Returning to the C.1−C.15 moiety of MTX, we were curious to test whether two structural moieties spaced by only two methylene groups could be treated independently, in order to determine its relative stereochemistry by synthesizing only 18 diastereomers instead of 128, i.e., eight diastereomers possible for model **C**, eight diastereomers possible for model **D**, and two remote diastereomers. At the same time, however, we still hoped that some residual chemical communication between the left and right halves of this portion of MTX could be detected by currently available spectroscopic means. In this context, it should be noted that even a trace amount of the natural product was not available for our work, and we solely depended on the published NMR data to conclude the complete relative stereochemical assignment.[12]

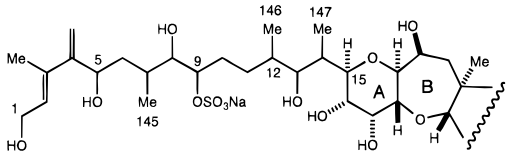

C.1-C.15 partial structure of MTX

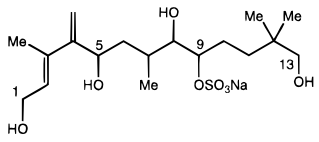

C

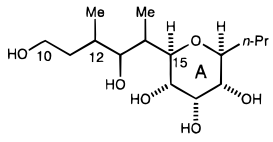

D

In order to test this experimentally, models **C** and **D** were chosen to represent the C.1−C.11 and C.11−C.15 portions, respectively. Scheme 2 summarizes the synthesis of all diastereomers possible for **C**. The relative and absolute stereochemistry at C.7 and C.8 was set by using the Roush boronate chemistry.[13] The reaction of the (*E*)-(*R*,*R*)-crotylboronate with the aldehyde **2**[14] was predicted to yield **3** preferentially. Indeed, this pair of reagent and substrate led almost exclusively to a single diastereomer. The olefin **3** was converted to the aldehyde **4**, which was then coupled with vinyllithium, to yield a 1:1.2 mixture of the two expected allylic alcohols **5** and **6**, which

Scheme 2[a]

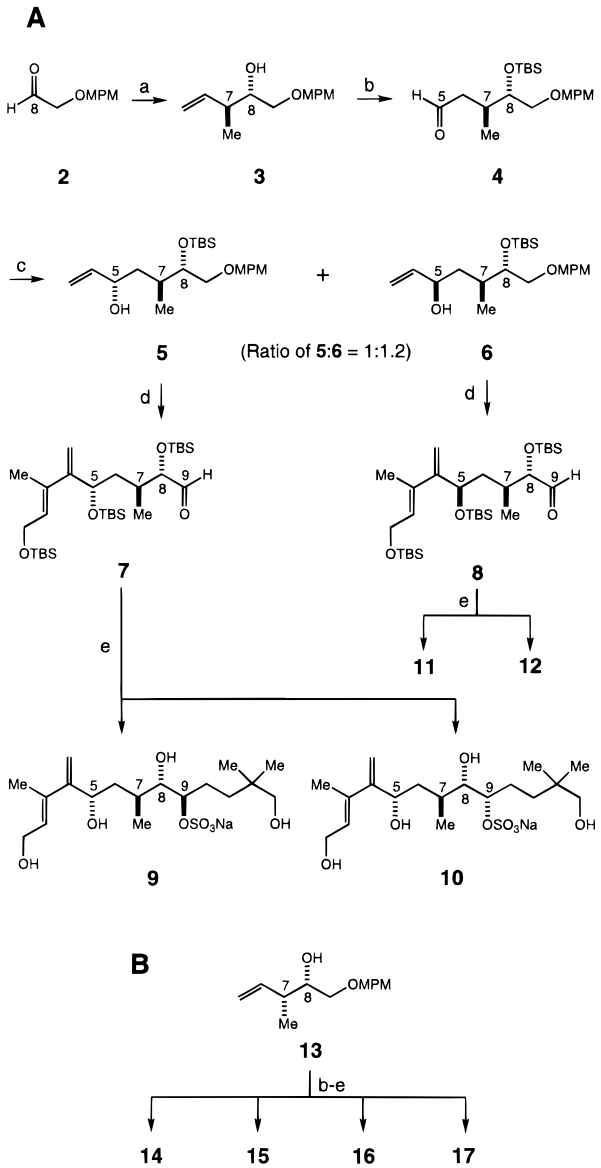

[a] (a) *(E)-(R,R)*-Crotylboronate, 4 Å molecular sieves, PhMe, −78 °C, 79%; (b) (1) TBSOTf, pyr, CH_2Cl_2, 23 °C; (2) catecholborane, $RhCl(PPh_3)_3$, THF, 23 °C;[64] 10% NaOH, H_2O_2, 23 °C; (3) $(COCl)_2$, DMSO, Et_3N, CH_2Cl_2, −78 °C; (c) vinyllithium, THF, −78 °C, 3 h, 0 °C, 10 min, 79% over four steps; (d) (1) TBSOTf, pyr, CH_2Cl_2, 23 °C; (2) OsO_4, NMO, EtOH−THF−H_2O (1:2:1), 23 °C, 16 h; $NaIO_4$, 23 °C, 24 h, 76% over two steps; (3) *(E)*-4-(*tert*-butyldimethylsiloxy)-2-buten-2-yl)lithium,[65] THF, −78 °C, 30 min; (4) $(COCl)_2$, DMSO, Et_3N, CH_2Cl_2, −78 °C, 88% over two steps; (5) DDQ, CH_2Cl_2−pH 7 buffer (10:1), 23 °C, 1 h, 80%; (6) $Ph_3P{=}CH_2$, pentane, 0 °C, 90 s, 67%; (7) $(COCl)_2$, DMSO, Et_3N, CH_2Cl_2, −78 °C, 96%; (e) (1) (4-(1-ethoxyethoxy)-3,3-dimethylbutyl)lithium,[66] THF, −78 °C, 15 min, 85%; (2) SO_3·pyr, pyr, 23 °C, 15 h;[67] (3) HF·pyr,[68] MeOH, 23 °C, 48 h, 89% over two steps.

(12) Yasumoto and co-workers completed an astonishing work to make the proton and carbon chemical shift assignment for each atom with 0.01 and 0.1 decimal place accuracy, respectively.[6]

(13) (a) Roush, W. R.; Walts, A. E.; Hoong, L. K. *J. Am. Chem. Soc.* **1985**, *107*, 8186−8190. (b) Roush, W. R.; Palkowitz, A. D.; Ando, K. *J. Am. Chem. Soc.* **1990**, *112*, 6348−6359 and references cited therein.

(14) England, P.; Chun, K. H.; Moran, E. J.; Armstrong, R. W. *Tetrahedron Lett.* **1990**, *31*, 2669−2672.

were chromatographically separated. The relative and absolute configuration of **5** and **6**, consequently of **3**, was established via NMR analyses of their cyclic derivatives, and the optical purity of **3** was estimated to be approximately 70−80%.[15]

The diastereomers **5** and **6** were subjected to the seven-step transformation, i.e., (1) protection of the C.5 alcohol, (2) oxidative cleavage of the vinyl group to generate the C.4 aldehyde, (3) coupling with the lithium reagent to form the C.3−C.4 bond, (4) oxidation of the resultant allylic alcohol to form the enone, (5) deprotection of the C.9 alcohol, (6) olefination to form the diene, and (7) oxidation of the C.9 alcohol to form the C.9 aldehydes. Each of the aldehydes **7** and **8** was then subjected to the next carbon−carbon bond forming reaction to yield the two possible C.9 diastereomers, which were separated by chromatography. Nuclear Overhauser effect (NOE) experiments with the C.8 and C.9 acetonides, prepared from both diastereomers, established their C.9 stereochemistry.[16] Each diastereomer was then subjected to sulfation at C.9, followed by deprotection, to furnish the four diastereomers **9**−**12**. Following the same sequence of reactions on the *syn*-adduct **13**, obtained from the reaction of **2** with (*Z*)-(*R,R*)-crotylboronate, the remaining four diastereomers **14**−**17** were also obtained (Scheme 2B).

All of the eight diastereomers were subjected to ^{1}H and ^{13}C NMR studies. Charts 1 and 2 show the difference in the chemical shifts of protons and carbons between MTX[12] and each diastereomer synthesized. This exercise clearly demonstrated that (1) each diastereomer exhibited distinct spectroscopic characteristics differing from the others, and (2) only the diastereomer **9** displayed spectroscopic characteristics that were virtually identical to those of MTX, therefore establishing that the relative stereochemistry of the C.1−C.11 portion of MTX is represented by that of **9**.

Model **D** was chosen for the study of the spectroscopic characteristics of the C.11−C.15 portion of MTX. Scheme 3 outlines the synthesis of the C.13−C.19 portion from the aldehyde **18**,[17] readily available from D-ribose. Addition of the allyl group was best achieved by the reaction of allylindium bromide with **18** to yield a 6:1 mixture of the two possible diastereomers. The major product was tentatively assigned to be the desired diastereomer, which was confirmed later (see Scheme 4). The major diastereomer was then converted into the aldehyde **19**. Addition of the Roush (*Z*)-*(R,R)*-crotylboronate to **19** furnished the expected product **20** exclusively, whereas addition of the corresponding (*Z*)-*(S,S)*-reagent gave 1.5:1 mixtures of **20** and **21**. Similarly, addition of (*E*)-*(R,R)*- and (*E*)-*(S,S)*-crotylboronates to **19** yielded a 9:1 and 1:1.2 mixture of **22** and **23**, respectively.

On the basis of the precedents of Roush's work,[13] the exclusive product formed with (*Z*)-*(R,R)*-crotylboronate was anticipated to be **20**, whereas the major product formed with (*E*)-*(R,R)*-crotylboronate was expected to be **22**. Thus, **20** and **22** should have the same stereochemistry at C.14 but the opposite stereochemistry at C.15, which was confirmed from the following experiments (Scheme 4). Oxidation of the C.15 hydroxy group of **20**, deprotection of the C.19 alcohol, and reductive cyclization furnished exclusively the expected C.15 equatorial product **26**; the vicinal proton coupling constants ($J_{15,16}$ = 9.7 Hz and $J_{18,19}$ = 9.5 Hz) observed for **26** led to the conclusion that the C.15 and C.19 substituents were equatorial. The same sequence of reactions on **22**, the major product formed by the reaction of (*E*)-*(R,R)*-crotylboronate with **19**, also furnished the identical equatorial product **26**. Since **20** was formed from *(Z)*-crotylboronate and **22** was formed from *(E)*-crotylboronate, their C.14 and C.15 relative stereochemistry should be *syn* and *anti*, respectively.

This conclusion was further supported by two additional experiments. First, **20** gave exclusively **26** via the alternative mode of reductive cyclization, i.e., **20** → **25** → **26**; the C.15 stereochemistry of **20** was retained in this transformation,

Chart 1. Difference in Proton Chemical Shifts between MTX and Each of **9**−**12** and **14**−**17** (500 MHz, 2:1 CD_3CN-D_2O)[a]

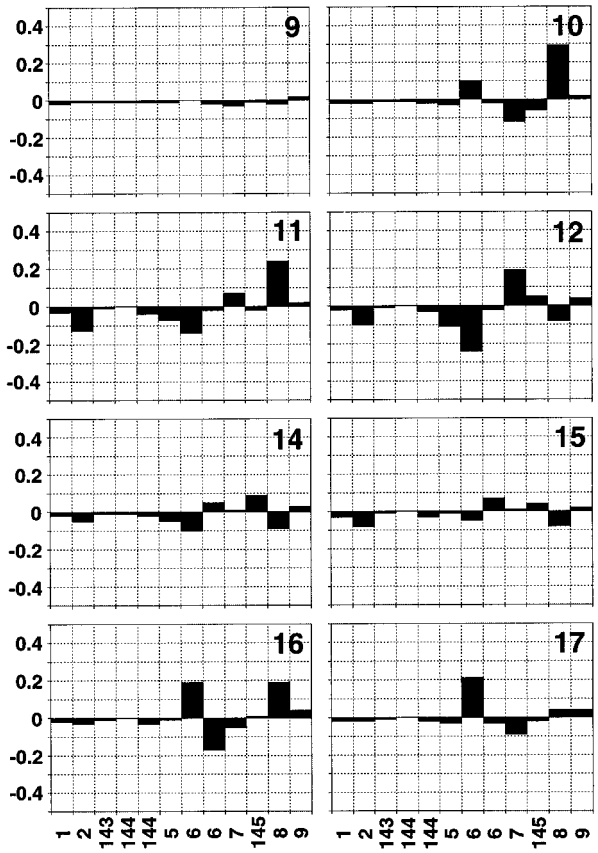

[a] The *x*- and *y*-axes represent carbon number and Δδ (Δδ = δ_{MTX} − $\delta_{SyntheticModel}$ in ppm), respectively, for all the charts in this paper.

(15) The absolute configuration and optical purity of **3** were established via its transformation into the Mosher ester of 2-methyl-1-butanol and comparison of it with the corrresponding Mosher ester prepared from (*S*)-(−)-2-methyl-1-butanol (Aldrich). The relative stereochemistry of **5** and **6** was established via the NMR study of the cyclic compounds **i** and **ii**, prepared from them in four steps, i.e., (1) BnBr/NaH, (2) TBAF, (3) OsO_4/$NaIO_4$, and (4) Ac_2O/pyr. At the early phase of the work, the mixture of **5** and **6** was used for the following transformation. However, using the pure materials, **5** and **6** were demonstrated to yield **7** and **8**, respectively.

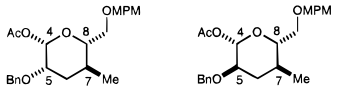

i : $J_{4,5}$ = 1.4 Hz, $J_{7,8}$ = 9.7 Hz **ii** : $J_{4,5}$ = 8.0 Hz, $J_{7,8}$ = 10.1 Hz

(16) The relative configuration of **9** and **10** was established from the NOE experiments of the acetonides **iii** and **iv**, prepared in three steps, i.e., (1) pyr/dioxane/120 °C, (2) $MeC(OMe)_2Me$/PPTS, and (3) Ac_2O/pyr. The acetonide **iii** exhibited clear cross peaks between the C.8/C.9 and C.7/C.10 protons, whereas the acetonide **iv** did not show the corresponding cross peaks but did show cross peaks between the C.7/C.9 and C.9/C.145 protons.

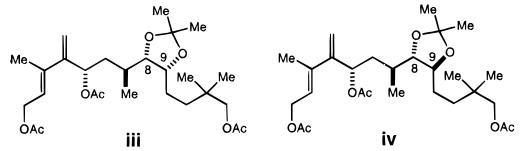

(17) Tadano, K.; Maeda, H.; Hoshino, M.; Iimura, Y.; Suami, T. *J. Org. Chem.* **1987**, *52*, 1946−1956.

Chart 2. Difference in Carbon Chemical Shifts between MTX and Each of **9**−**12** and **14**−**17** (125 MHz, 2:1 CD_3CN-D_2O)

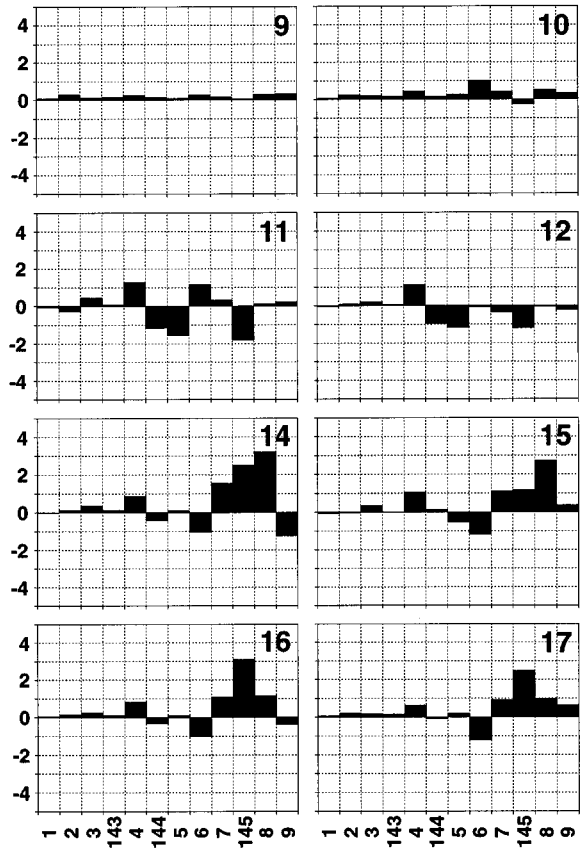

whereas the C.19 stereochemistry was retained in the previous mode of reductive cyclization. Second, the major *anti*-product **23**, obtained with the *(E)-(S,S)*-crotylboronate, furnished exclusively **28** in the three-step sequence of reductive cyclization (Scheme 4B). The vicinal proton coupling constants ($J_{15,16}$ = 9.7 Hz and $J_{18,19}$ = 9.5 Hz) demonstrated that the C.15 and C.19 substituents of **28** were equatorial, and consequently **28** was the C.14 diastereomer of **26**. These results were consistent with the conclusion derived from the previous experiments.

The Roush crotylboronate chemistry should allow the addition of the next propionate unit to **26** and **28**. However, it was difficult to predict the influence of the pre-existing stereocenters on the overall stereochemical outcome.[18] The aldehydes **29** and **38**, derived from **26** and **28**, respectively, were subjected to *(E)-(R,R)*, *(E)-(S,S)*-, *(Z)-(R,R)*-, and *(Z)-(S,S)*-crotylboronates, followed by hydroboration and deprotection, to yield the expected products (Scheme 5). All of the possible diastereomers **34**−**37** were obtained from the aldehyde **29**, whereas only two diastereomers **43** and **44** were obtained from the aldehyde **38**.

While these observations were intriguing, it was necessary to obtain the remaining two diastereomers for the present work, which was accomplished as summarized in Scheme 6. The conjugate reduction of the enone **45**, followed by hydride reduction and deprotection of the TBS and benzyl group, gave a 1.0:1.9:1.6:1.0 mixture of the four possible diastereomers **43**, **44**, **46**, and **47**. The last two products corresponded to the diastereomers not obtained in the previous experiments.

All of the eight diastereomers were subjected to ^1H and ^{13}C NMR studies. Charts 3 and 4 show the difference in the

(18) For a review of double stereodifferentiation, for example, see: Masamune, S.; Choy, W.; Petersen, J. S.; Sita, L. R. *Angew. Chem., Int. Ed. Engl.* **1985**, *24*, 1−76.

Scheme 3[a]

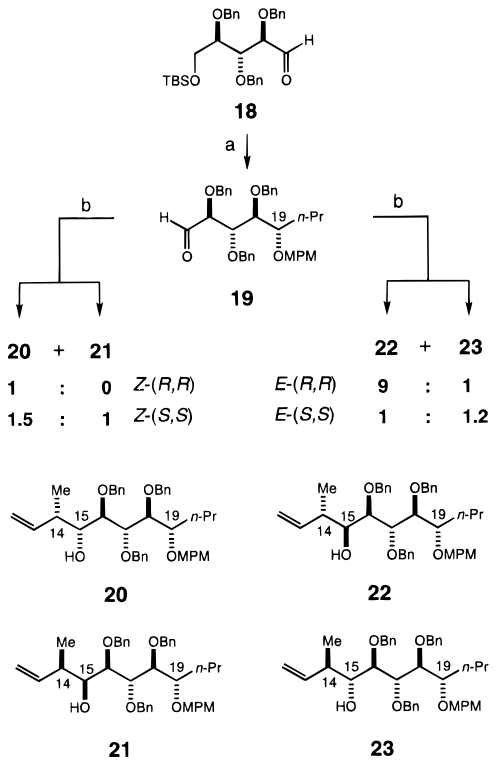

[a] (a) (1) Allyl bromide, In, DMF, 23 °C, ratio of α:β = 6:1, 85%;[69] (2) H_2, Lindlar catalyst, EtOAc, 23 °C, overnight; (3) NaH, MPMCl, DMF, 23 °C, 12 h; (4) *n*-Bu_4NF, THF, 50 °C, 30 min, 84% over three steps; (5) $(COCl)_2$, DMSO, Et_3N, CH_2Cl_2, −78 °C, 92%; (b) crotylboronate, 3 Å molecular sieves, PhMe, −78 °C.

Scheme 4[a]

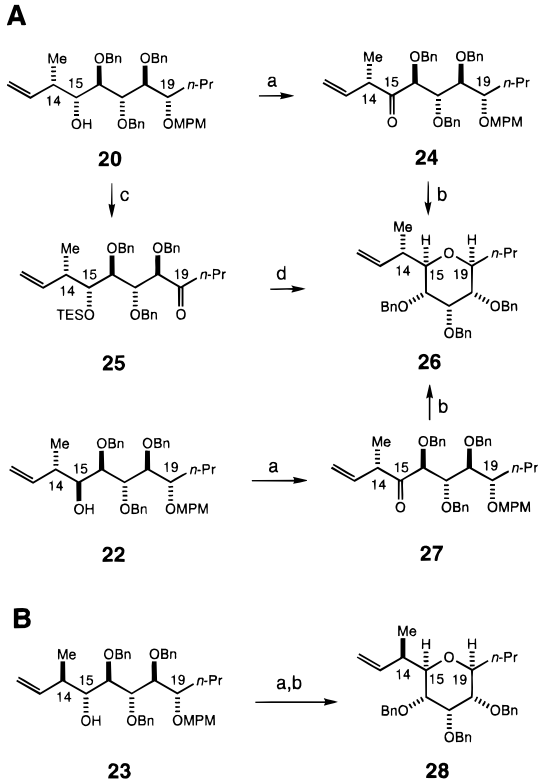

[a] (a) $(COCl)_2$, DMSO, Et_3N, CH_2Cl_2 −78 °C; (b) (1) DDQ, CH_2Cl_2−H_2O (10:1), 23 °C, 1 h; (2) BF_3·OEt_2, Et_3SiH, CH_3CN−CH_2Cl_2 (10:1), −20 °C, 15 min; 75% over three steps; (c) (1) TESOTf, 2,6-lutidine, CH_2Cl_2; (2) DDQ, CH_2Cl_2−H_2O (10:1), 23 °C, 1 h, 80% over two steps; (3) $(COCl)_2$, DMSO, Et_3N, CH_2Cl_2, −78 °C, 72%; (d) (1) HF·pyr, THF, 23 °C, 3 h, 76%; (2) same as step b2, 82%.

Scheme 5[a]

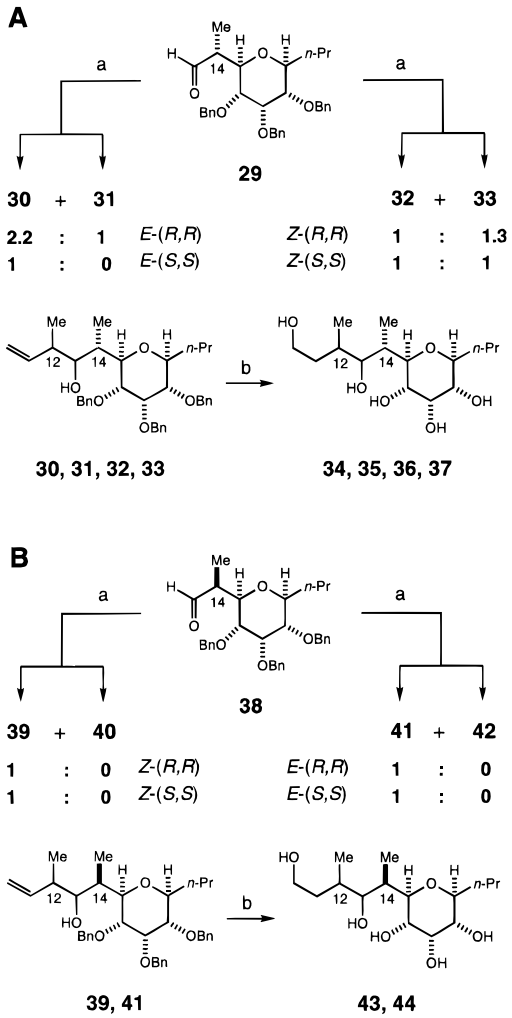

[a] (a) Crotylboronate, 4 Å molecular sieves, PhMe, −78 °C; (b) (1) catecholborane, $RhCl(Ph_3P)_3$ (cat.), THF, 0−23 °C, 1 h; 10% NaOH, 30% H_2O_2, 0−23 °C, 3 h, 80%; (2) H_2, $Pd(OH)_2$ on C (cat.), EtOH, 23 °C, 3 h, 99%.

Scheme 6[a]

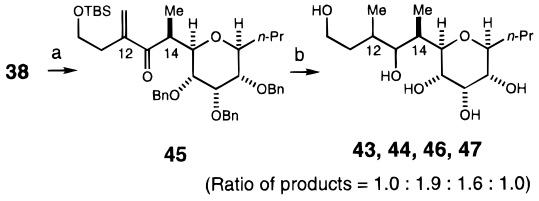

[a] (a) (1) 4-(*tert*-Butyldimethylsiloxy)-1-buten-2-yl iodide,[70] 1% $NiCl_2$/$CrCl_2$, THF−DMF (2:1), 23 °C, 23 h; (2) $(COCl)_2$, DMSO, Et_3N, CH_2Cl_2, −78 °C, 33% over two steps (48% recovered aldehyde **38**); (b) (1) $(CuH{\cdot}PPh_3)_6$, wet PhH, 23 °C, 3 h, ratio of α:β at C.12=1:1, 89%;[71] (2) DIBAL, CH_2Cl_2, −78 °C, 0.5 h, then 23 °C, 10 min, 85%; (3) *n*-Bu_4NF, THF, 23 °C, 1 h, 95%; (4) H_2, $Pd(OH)_2$ on C (cat.), EtOH, 23 °C, 3 h, 95%.

chemical shifts for protons and carbons between MTX and each of the diastereomers synthesized. This exercise once again demonstrated that (1) each diastereomer exhibited distinct spectroscopic characteristics differing from the others and (2) only diastereomer **35** displayed spectroscopic characteristics that were virtually identical to those of MTX.

The C.12 and C.13 stereochemistry of **35** was then addressed. As noted earlier (Scheme 5), addition of *(E)-(R,R)*-crotylboronate to the aldehyde **29** yielded the two expected products in a 2.2:1 ratio. Therefore, the C.12 and C.13 stereochemistry of

Chart 3. Difference in Proton Chemical Shifts between MTX and Each of **34**−**37**, **43**, **44**, **46**, and **47** (500 MHz, 2:1 CD_3CN-D_2O)

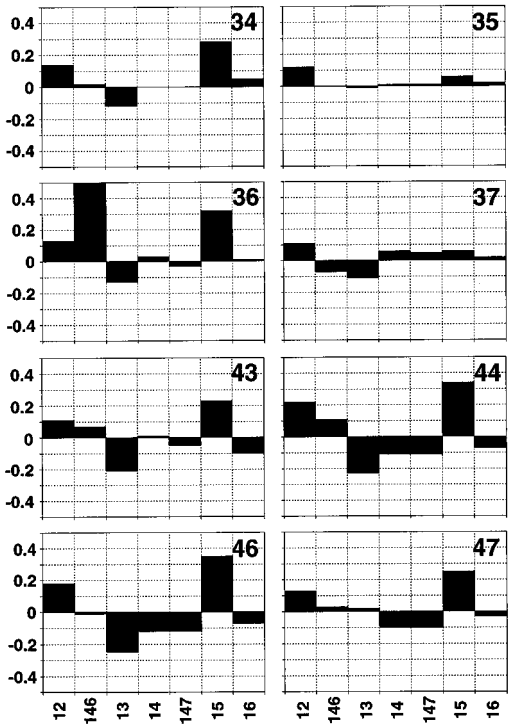

Chart 4. Difference in Carbon Chemical Shifts between MTX and Each of **34**−**37**, **43**, **44**, **46**, and **47** (125 MHz, 2:1 CD_3CN-D_2O)

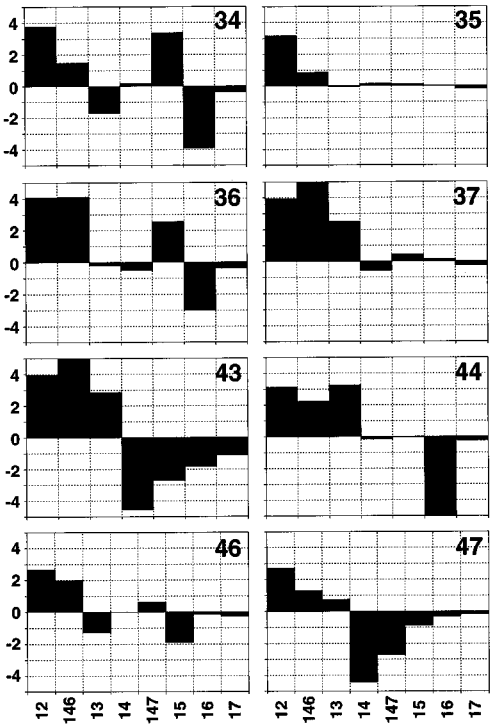

these products should be *anti*, and they should correspond to either **30** and **31** or vice versa. The major product **30** was subjected to a sequence of degradation reactions,[19] which furnished the triol **49** (Scheme 7). Seven well-separated signals

(19) This degradation was carried out according to the protocol used in the palytoxin case: Ko, S. S.; Finan, J. M.; Yonaga, M.; Kishi, Y.; Uemura, D.; Hirata, Y. *J. Am. Chem. Soc.* **1982**, *104*, 7364−7367.

Scheme 7[a]

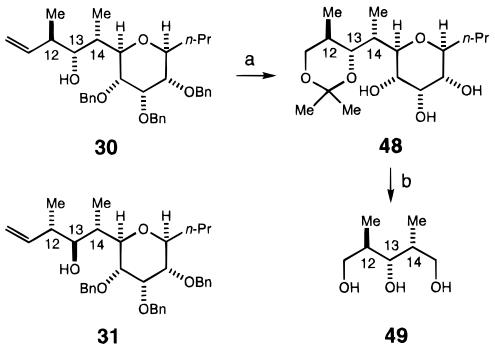

[a] (a) (1) O_3, −78 °C, MeOH; $NaBH_4$, 94%; (2) $MeC(OMe)_2Me$, *p*-TsOH (cat.), 23 °C, 1 h; (3) H_2, $Pd(OH)_2$ on C (cat.), EtOAc, 52% over two steps; (b) (1) $NaIO_4$, THF−pH 7 buffer (1:1), 23 °C, 0.5 h; (2) MCPBA, CH_2Cl_2−pH 7 buffer (2:1), 23 °C, 5 h; (3) LAH, THF, 23 °C, 0.5 h; (4) MeOH, *p*-TsOH (cat.), 23 °C, 2 h, 46% over four steps.

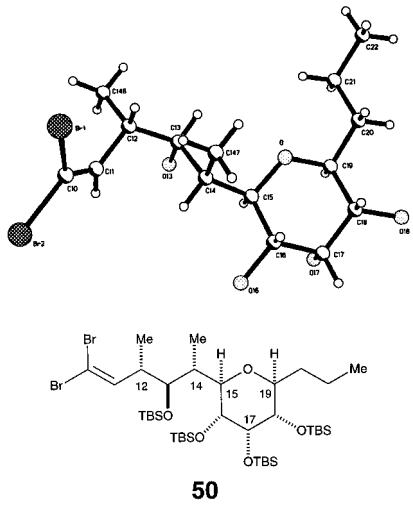

Figure 2. Crystal structure of **50**. The TBS groups in the ORTEP representation were removed for clarity.

were observed in its ^{13}C NMR spectrum,[20] establishing the relative stereochemistry for **49**, and consequently that for **30**. This conclusion was further supported by a single crystal X-ray analysis of **50** derived from **31** (Figure 2).[21] These experimental results established that the relative stereochemistry of the C.12−C.15 portion of MTX is represented by that of **50**.

Having established the relative stereochemistry for both the C.1−C.11 and C.11−C.15 portions, we planned to synthesize the two possible remote diastereomers **51** and **52**, and to compare their spectroscopic characteristics with those of MTX. Obviously, the olefin **31** (Scheme 7) was an ideal starting material for this synthesis, but one practical problem had to be addressed, i.e., **31** was obtained only as the minor product via the crotylboronate chemistry. Among several reagents and conditions tested, the addition of the zinc reagent prepared from crotyl bromide to the aldehyde **29** in THF at −93 °C gave the most satisfactory result.[22] The method to construct the two remote diastereomers was then studied, and the synthetic route shown in Scheme 8 met our requirements,[23] including material throughput and, more importantly, unambiguous stereochemical assignment of the newly introduced chiral center at C.9. The first carbon−carbon bond formation was accomplished by coupling of the aldehyde **53** with the dibromo olefin **50**, to yield an easily separable 1.5:1 mixture of the two expected products **54** and **55**. The acetylenic bond in **54** and **55** provided a useful handle to establish the stereochemistry of the newly introduced chiral center via degradation reactions.[24]

Formation of the C.3−C.4 bond was achieved by coupling the aldehyde **56**, derived from **54**, with the lithium reagent prepared from (*E*)-4-(*tert*-butyldimethylsiloxy)-2-buten-2-yl bromide.[25] Oxidation of the resultant allylic alcohol and deprotection of the C.9 alcohol provided the enone **57**. Wittig reaction, sulfation of the C.9 alcohol, and deprotection of all the silyl protecting groups furnished the final product **51**, which

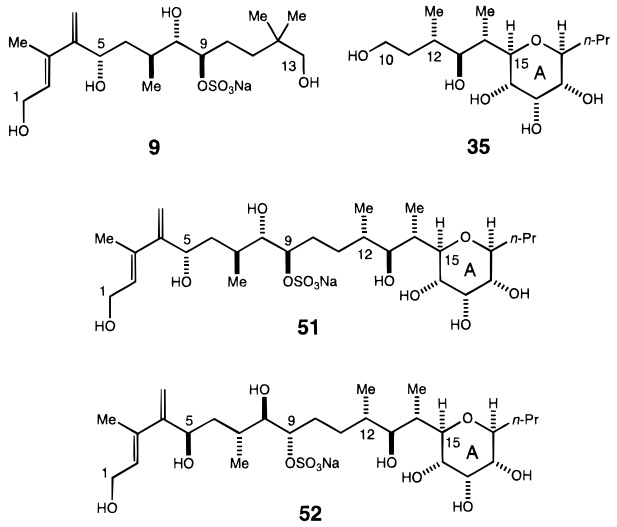

was isolated as its sodium salt by silica gel column chromatography. Using the same chemistry but with **59**, the antipode of **53**, the remote diastereomer **52** was also synthesized (Scheme 8B).

The two remote diastereomers **51** and **52** were subjected to NMR studies. Charts 5 and 6 summarize the difference in the chemical shifts observed between MTX and the remote diastereomers. As expected, both the remote diastereomers **51** and **52** were found to exhibit NMR characteristics, particularly ^{13}C NMR, very similar to each other, and very similar to the NMR characteristics of MTX in that region.[26] However, upon close examination of their ^1H NMR spectra, small but significant differences were detected between **51** and **52** and also between **52** and MTX. It is important to recognize that the differences

(20) ^{13}C NMR (125 MHz, $CDCl_3$) δ 75.4 ppm, 66.8, 66.6, 39.5, 38.7, 14.0, 9.7.

(21) We thank Dr. A. Marcus Semones in this group for this X-ray analysis.

(22) Zn(0), Cr(II), and In(0) were tested in several solvent systems at a wide range of temperatures. Among them, Zn(0) in THF at −93 °C yielded a 51:35:9:5 mixture (^1H NMR) of the products, with the major product being the desired **31** and the second major product being **30**. The desired product **31** was isolated in 44% yield on a preparative scale.

(23) In the model **C** series, the C.9−C.10 bond was formed by coupling the aldehyde with the alkyllithium reagent. However, in the model **51**/**52** series, the attempted preparations of the corresponding lithium reagent failed. The coupling of the acetylene anion prepared from **50** with the complete C.1−C.9 aldehyde was very efficient, but the selective reduction of the acetylene over the diene proved problematic.

(24) The relative configuration of **54** and **55** was established from the vicinal coupling constants observed for the bis-acetonides **v** and **vi**, prepared from them in 5 steps, i.e., (1) H_2/Lindlar catalyst, (2) $BnOC(=NH)CCl_3$/TfOH, (3) O_3, followed by $NaBH_4$, (4) HCl (cat.)/aqueous MeOH, and (5) $MeC(OMe)_2Me$/PPTS.

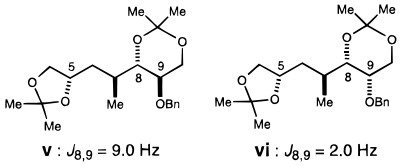

(25) Meyer, S. D.; Miwa, T.; Nakatsuka, M.; Schreiber, S. L. *J. Org. Chem.* **1992**, *57*, 5058−5060.

Scheme 8[a]

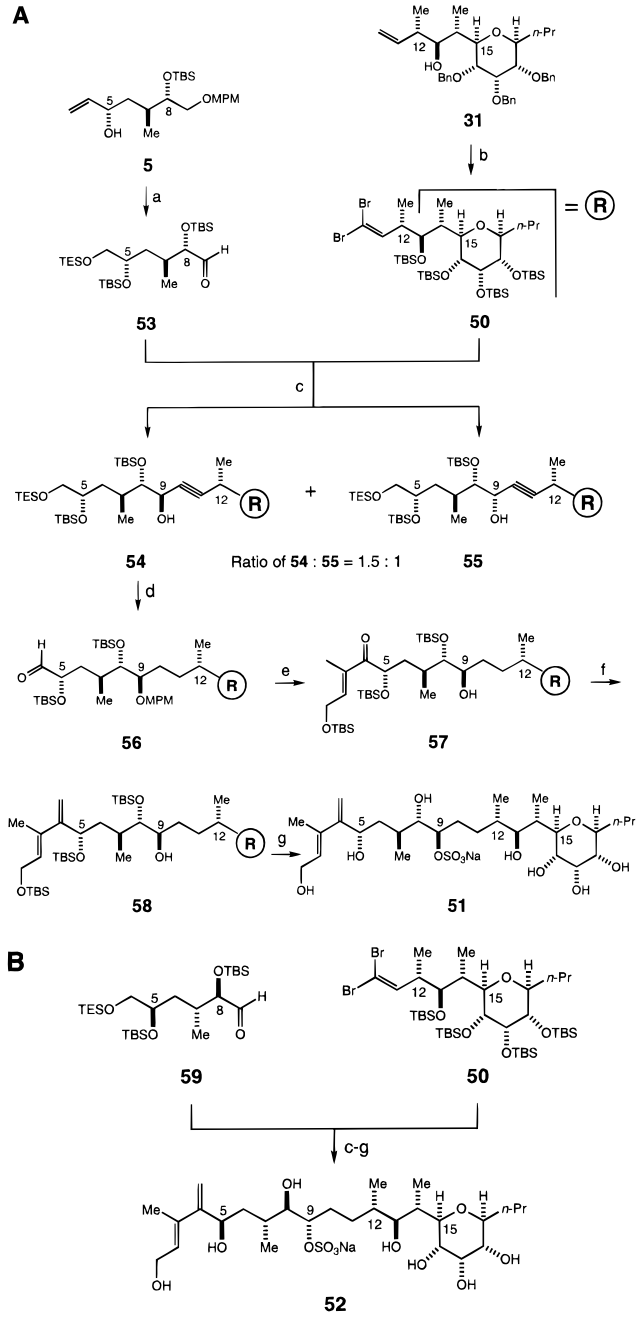

[a] (a) (1) TBSOTf, Et_3N, CH_2Cl_2, 98%; (2) O_3, CH_2Cl_2−MeOH−pyr (10:5:0.3); $NaBH_4$, 78%; (3) TESCl, Et_3N, DMAP (cat.), CH_2Cl_2, 23 °C, 1 h, 96%; (4) H_2, $Pd(OH)_2$ on C (cat.), EtOAc, 23 °C, 1 h, 90%; (5) $(COCl)_2$, DMSO, Et_3N, CH_2Cl_2, −78 °C, 79%; (b) (1) Na, NH_3, −33 °C, 1 h, 100%; (2) TBSCl, $AgNO_3$, pyr, DMF, 23 °C, 12 h, 86%; (3) TBSOTf, *i*-Pr_2NEt, CH_2Cl_2, 23 °C, 42 h, 88%; (4) O_3, CH_2Cl_2−MeOH (12:1), −78 °C; $NaBH_4$, 23 °C, 1 h, 82%; (5) $(COCl)_2$, DMSO, Et_3N, CH_2Cl_2, −78 °C, 99%; (6) $PhHgCBr_3$, PPh_3, PhH, 80 °C, 1 h, 97%;[72] (c) **50**, *n*-BuLi, −78 °C, 1 h, then 0 °C, 6 min, −78 °C; **53**, 25 min, 97%; (d) (1) H_2, 1% Rh on Al_2O_3 (cat.), EtOAc, 100%; (2) *p*-methoxybenzyl 2,2,2-trichloroacetimidate, TfOH (trace), Et_2O, 23 °C, 12 h, 37% (60% recovered starting material); (3) PPTS, MeOH−Et_2O (3:2), 23 °C, 0.5 h, 93%; (4) $(COCl)_2$, DMSO, Et_3N, CH_2Cl_2, −78 °C, 85%; (e) (1) ((*E*)-4-*tert*-butyldimethylsiloxy)-2-buten-2-yl)lithium, THF, −78 °C, 20 min; (2) $(COCl)_2$, DMSO, Et_3N, CH_2Cl_2, −78 °C, 76% over two steps; (3) DDQ, CH_2Cl_2−pH 7 buffer (10:1), 23 °C, 40 min, 90%; (f) (1) CH_2═CHOEt, PPTS, CH_2Cl_2, 23 °C, 6 h, 95%; (2) Ph_3P═CH_2, pentane, 0 °C, 3 h, 76%; (3) PPTS, Et_2O−MeOH (3:1), 23 °C, 6 h; (4) TBSCl, Et_3N, DMAP, CH_2Cl_2, 23 °C, 2.5 h, 86% over two steps; (g) (1) SO_3·pyr, pyr, 23 °C, 12 h, 96%; (2) HF−pyr, MeOH, 23 °C, 20 days, 79%.

Chart 5. Difference in Proton Chemical Shifts between MTX and Each of **51** and **52** (500 MHz, 1:1 C_5D_5N−CD_3OD)

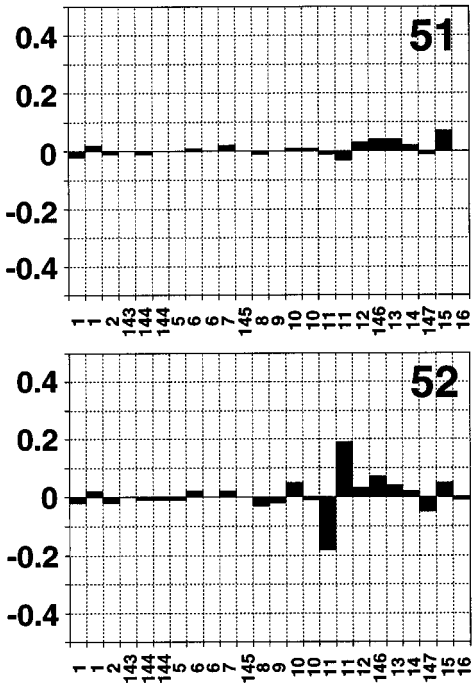

Chart 6. Difference in Carbon Chemical Shifts between MTX and Each of **51** and **52** (125 MHz, 1:1 C_5D_5N−CD_3OD)

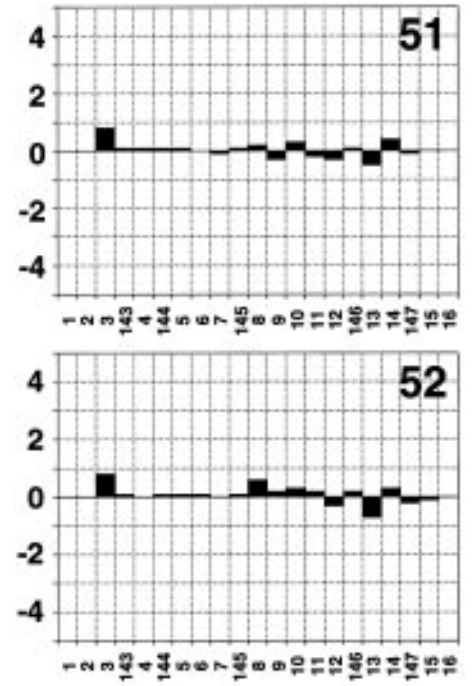

were particularly distinct in the chemical shifts of the protons in the bridging area between the two remote sides.[27] This being

(26) We thank Professor Murata for information on the revised assignment of the carbon chemical shift for the C.12 methyl group (δ 18.0 ppm). The chemical shift for the C.3 carbon of MTX[6] appears to have been misassigned.

(27) We chose a geminal dimethyl group at the C.12 position of model **C**, in order to simplify the spectroscopic analysis. Interestingly, we observed that the geminal dimethyl groups of **9** exhibited a small but distinct diastereotopic property in its ^1H NMR spectrum, which was the first sign of the presence of some detectable residual communication between the two halves.

recognized, it became evident that the remote diastereomer **51** represents the stereochemistry of the corresponding moiety of MTX.[28]

The experimental results given in this section provided the answers to the two questions raised earlier. Although bridged by only two methylene groups, the left-side and right-side moieties could still be treated independently, yet small but distinct communications between these two moieties were detected by currently available spectroscopic means, which allowed the assignment of the relative stereochemistry of the C.1−C.15 portion of MTX.

2. C.35−C.39 Acyclic Portion. The C.35−C.39 portion of MTX contained two unassigned chiral centers on the acyclic backbone. It is important to note that, in order to establish the complete relative stereochemistry of MTX, their configuration relative not only to C.35 but also to C.39 must be determined. By this means, the relative stereochemistry at the remote positions, for example C.35 and C.39, can be established. We decided to address these questions via (1) the selection of a model properly representing this portion of MTX; (2) the synthesis of all the possible diastereomers with respect to the C.35, C.36, C.37, and C.39 chiral centers; (3) the comparison of the NMR characteristics of each diastereomer with those of MTX; and (4) the identification of which diastereomer represents the spectroscopic properties of the corresponding part of MTX. Unlike the C.1−C.15 moiety, the chiral centers present in this region are in close proximity to each other so that each diastereomer should exhibit spectroscopic characteristics differing from those of the others. We chose model **E**, which contained the four chiral centers in question. This strategy called for the synthesis of eight possible diastereomers.[29]

The synthetic plan of all of the eight diastereomers is outlined in Scheme 9. Several comments are in order: (1) the four diastereomers **72**−**75** could be prepared via the acetylene **64**, i.e., reduction of **64** selectively into the *cis*- or *trans*-olefin **65**

(28) In order to eliminate the possibility that any electronic and/or steric factor might give an unforeseen effect on their proton and carbon NMR spectra, we synthesized two additional models, **vii** and **viii**, both of which exhibited NMR characteristics very similar to those of **51**, and **vii** is even closer to those of MTX than **51**. Below is depicted the difference in proton (500 MHz, 1:1 C_5D_5N−CD_3OD) and carbon (125 MHz, 1:1 C_5D_5N-CD_3-OD) chemical shifts between MTX and each of **vii** and **viii**. The *x*- and *y*-axes represent carbon number and $\Delta\delta$ ($\Delta\delta = \delta_{MTX} - \delta_{SyntheticModel}$ in ppm), respectively.

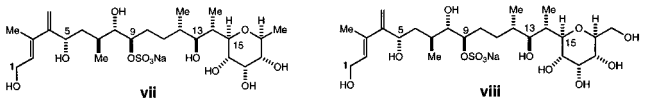

vii **viii**

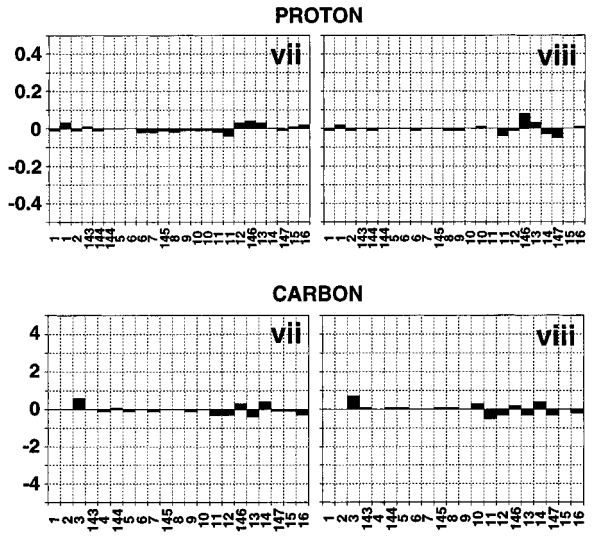

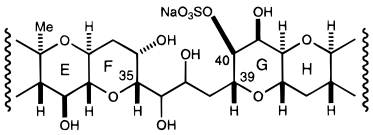

C.35-C.39 partial structure of MTX

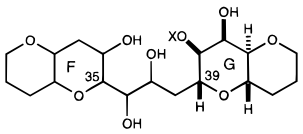

Ea : X = SO_3Na
Eb : X = H

or **66**, followed by dihydroxylation; (2) the acetylene **64** could stereoselectively be synthesized by coupling the lactone **62** with the acetylene anion generated from the dibromo olefin **63**, followed by silane reduction; (3) both **62** and **63** could be prepared from the common synthetic intermediate **61**; (4) the

Scheme 9

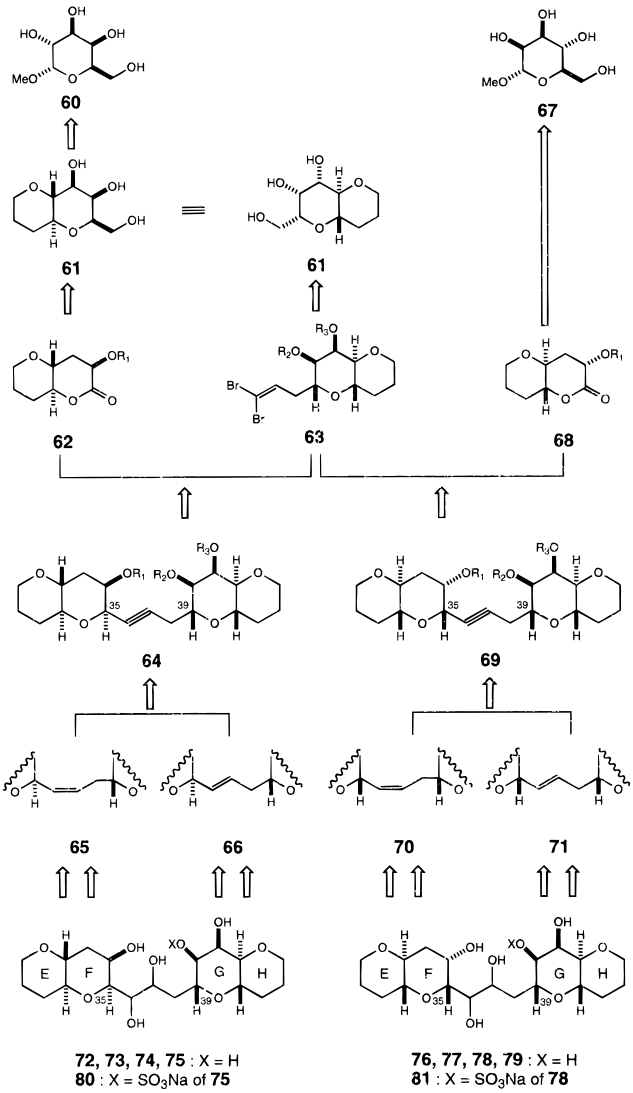

(29) Tachibana and co-workers recently reported the relative stereochemistry of this portion of MTX.[9] At the onset, they relied on the NMR data to select one diastereomer, corresponding to **81**, over the remaining seven diastereomers, and they synthesized that diastereomer to conclude the relative stereochemistry of this portion of MTX. It is interesting to note that **74** and **75** are the C.39 and C.35 diastereomers of **78**, respectively.

remaining four diastereomers **76**−**79** should be available via the same synthetic sequences but with the lactone **68**, the antipode of **62**.

Scheme 10 outlines the synthesis of the lactone **86** from **82**.[30] The silane reduction of the ketol, formed via addition of butenylmagnesium bromide to the lactone **82**, was expected to give the equatorial product **83**;[31] indeed, this reduction was highly stereoselective, yielding the desired equatorial product with a stereoselectivity greater than 20:1. The cyclization to form the second ring was best achieved by sodium hydride treatment of the pentol monomesylate **84**. The C.33 deoxygenation was effected by the Barton procedure,[32] and removal of the hydroxymethyl group to form the lactone was carried out in three steps.

Scheme 10[a]

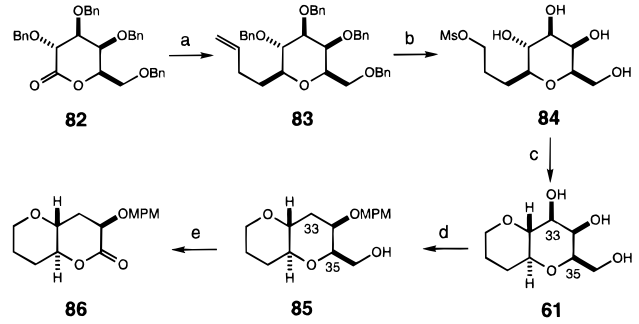

[a] (a) (1) 3-Buten-1-ylmagnesium bromide, Et_2O, −78 °C, 15 min, 91%; (2) Et_3SiH, $BF_3{\cdot}OEt_2$, CH_2Cl_2−CH_3CN (1:1), −20 °C, 15 min, 98%; (b) (1) O_3, MeOH−CH_2Cl_2 (2:1); $NaBH_4$, 88%; (2) MsCl, Et_3N, CH_2Cl_2, 0 °C, 15 min, 98%; (3) H_2, $Pd(OH)_2$ on C (cat.), MeOH, 23 °C, 4 h, 100%; (c) NaH, DMF, 23 °C, 12 h, 74%; (d) (1) *p*-MeOPhCH(OMe)$_2$, *p*-TsOH, DMF, 23 °C, vacuum, 12 h, 97%; (2) NaH, CS_2, MeI, THF, 23 °C, 30 min, 95%; (3) *n*-Bu_3SnH, AIBN, PhMe, 110 °C, 1 h, 75%; (4) DIBAL, CH_2Cl_2, −78 °C, 30 min, then 0 °C, 1 h, 98%; (e) (1) Ph_3P, imidazole, I_2, PhH, 70 °C, 3 h, 98%; (2) DBU, 1,2-dichlorobenzene, 200 °C, 15 min;[73] (3) O_3, MeOH, −78 °C; DMS, 23 °C, 1 h, 32% over two steps.

We planned to use the same triol **61**, an intermediate in the synthesis of the lactone **86**, for the synthesis of the dibromo olefin **90** as well (Scheme 11). For this purpose, it was necessary to invert the stereochemistry of both C.40 and C.41 alcoholic groups of **61**, which was effectively achieved via selective protection of the primary alcohol, olefin formation from the remaining *cis*-diol,[33] and then osmylation, to yield the desired diol **88** as the major product.

The synthesis of the lactone **96**, the antipode of **86**, from **91**[34] is summarized in Scheme 12. Once again, the cyclization to form the second ring was achieved with the tetraol monomesylate **92**. Although reductive cleavage of the anisylidene group[35] in **94** derived from the diol **93** was not selective, both regioisomers were usable for the synthesis of **96** by deoxygenation at C.33 under the Barton conditions, hydrolysis of the methyl glycoside, and oxidation of the resultant lactol to the lactone.

Scheme 11[a]

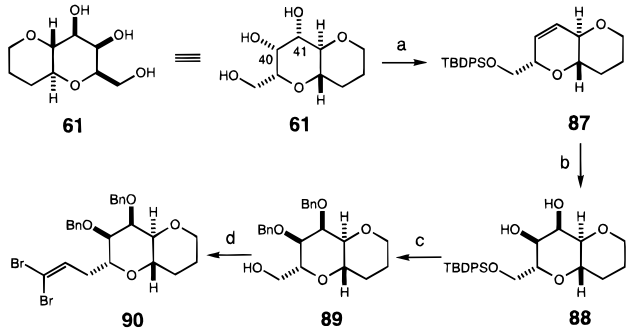

[a] (a) (1) TBSCl, DMAP, Et_3N, CH_2Cl_2, 23 °C, 3 days, 77%; (2) 1,1′-thiocarbonyldiimidazole, PhMe, 110 °C, 4 h, 95%; (3) 1,3-dimethyl-2-phenyl-1,3,2-diazaphospholidine, 23 °C, 3 h, 81%; (4) 1% HCl in 95% EtOH, 23 °C, 5 h, 96%; (5) TBDPSCl, imidazole, pyr, 23 °C, 11 h; (b) OsO_4, NMO, *t*-BuOH−acetone−H_2O (1:1:1), 23 °C, 48 h, 67% over two steps; (c) (1) BnBr, Ag_2O, Et_2O, 35 °C, 12 h; (2) BnBr, *n*-Bu_4NI (cat.), NaH, THF, 23 °C, 5 h; (3) 3% HCl in MeOH, 23 °C, 12 h, 72% over three steps; (d) (1) MsCl, Et_3N, CH_2Cl_2, 0 °C, 15 min, 96%; (2) NaCN, DMSO, 90 °C, 1.5 h, 98%; (3) DIBAL, PhMe, −78 °C, 10 min, 94%; (4) $PhHgCBr_3$, PhH, 80 °C, 1.5 h, 87%.

Scheme 12[a]

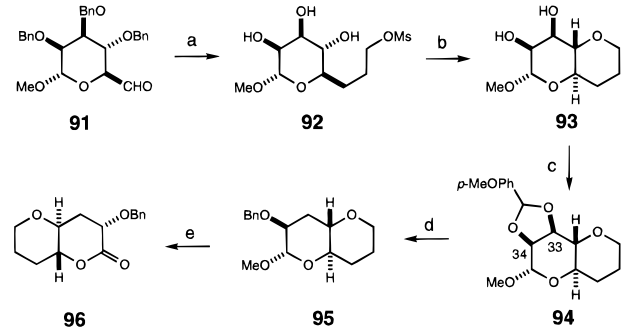

[a] (a) (1) $EtO_2CCH{=}PPh_3$, PhH, 23 °C, 2 h, 71%; (2) H_2, Lindlar catalyst, EtOAc, 23 °C, 16 h, 100%; (3) DIBAL, CH_2Cl_2, 0 °C, 15 min, 96%; (4) MsCl, Et_3N, CH_2Cl_2, 0 °C, 15 min, 99%; (5) H_2, $Pd(OH)_2$ on C (cat.), MeOH, 23 °C, 12 h, 100%; (b) NaH, DMF, 23 °C, 4 h, 92%; (c) *p*-MeOPhCH(OMe)$_2$, HBF_4, DMF, 23 °C, 12 h, 88%; (d) (1) DIBAL, CH_2Cl_2, 0 °C, 1 h, ratio of products = 1:1.3, 96%; (2) for the minor isomer, i.e., C.33-OMPM, NaH, *n*-Bu_4NI (cat.), BnBr, THF−DMF (3:1), 23 °C, 2.5 h, 93%; CAN, CH_3CN−H_2O (9:1), 23 °C, 40 min, 80%; NaH, imidazole (cat.), CS_2, MeI, THF, 90%; Bu_3SnH, AIBN, PhMe, 110 °C, 0.5 h, 63%; for the major isomer, i.e., C.34-OMPM: NaH, imidazole (cat.), CS_2, MeI, THF, 15 min, 93%; Bu_3SnH, AIBN, PhMe, 110 °C, 0.5 h, 61%; DDQ, CH_2Cl_2−H_2O (10:1), 23 °C, 40 min, 83%; BnBr, NaH, *n*-Bu_4NI (cat.), THF−DMF (3:1), 23 °C, 2.5 h, 76%; (e) (1) THF−CF_3CO_2H−H_2O (1:1:1), 65 °C, 26 h, 85%; (2) $(COCl)_2$, DMSO, Et_3N, CH_2Cl_2, −78 °C, 76%.

Coupling of the lactone **96** with the acetylene anion generated in situ from the dibromide **90**,[36] followed by silane reduction, gave once again the desired, equatorial acetylene **97** exclusively (Scheme 13). Partial reduction of the acetylene **97** (Lindlar catalyst) to the *cis*-olefin **98**, followed by osmylation, gave a 17:1 mixture of the two possible diols **99** and **100**. On the basis of the empirical rule,[37] their stereochemistry was tentatively assigned as indicated. The *trans*-olefin **101** was stereospecifically obtained from the acetylene **97** in three steps[38] and then subjected to osmylation, to yield a 6:1 mixture of the two possible diols **102** and **103**. Once again on the basis of the

(30) Dondoni, A.; Scherrmann, M.-C. *J. Org. Chem.* **1994**, *59*, 6404−6412.

(31) Lewis, M. D.; Cha, J. K.; Kishi, Y. *J. Am. Chem. Soc*. **1982**, *104*, 4976−4978.

(32) Barton, D. H. R.; McCombie, S. W. *J. Chem. Soc., Perkin Trans. 1* **1975**, 1574−1585. For a review on this subject, for example, see: Hartwig, W. *Tetrahedron* **1983**, *39*, 2609−2645.

(33) Corey, E. J.; Hopkins, P. B. *Tetrahedron Lett.* **1982**, *23*, 1979−1982.

(34) Barnes, J. C.; Brimacombe, J. S.; Kabir, A. K. M. S.; Weakley, T. J. R. *J. Chem. Soc., Perkin Trans. 1* **1988**, 3391−3397.

(35) Takano, S.; Akiyama, M.; Sato, S.; Ogasawara, K. *Chem. Lett.* **1983**, 1593−1596.

(36) Corey, E. J.; Fuchs, P. L. *Tetrahedron Lett.* **1972**, 3769−3772.

(37) (a) Cha, J. K.; Christ, W. J.; Kishi, Y. *Tetrahedron Lett.* **1983**, *24*, 3943−3946. (b) Christ, W. J.; Cha, J. K.; Kishi, Y. *Tetrahedron Lett.* **1983**, *24*, 3947−3950.

(38) Attempted photochemically- or radically-induced direct *cis*-to-*trans* isomerization gave no promising results.

Scheme 13[a]

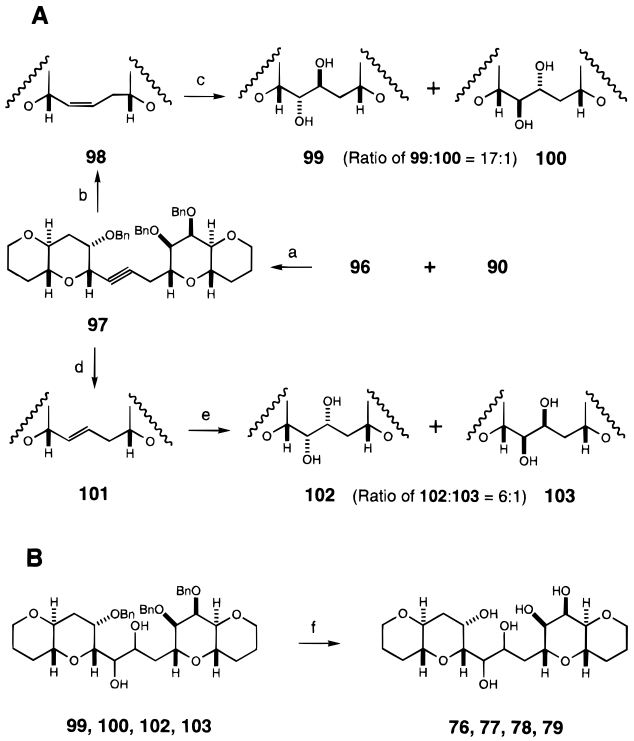

[a] (a) (1) *n*-BuLi, **90**, THF, −78 °C, 1 h, then 0 °C, 10 min; **96**, −78 °C, 0.5 h, then 23 °C, 95%; (2) Et_3SiH, $BF_3{\cdot}OEt_2$, $CH_2Cl_2-CH_3CN$ (1:1), −25 °C, 0.5 h, 83%; (b) H_2, Lindlar catalyst, EtOAc, 50 min, 61%; (c) OsO_4, NMO, *t*-BuOH−acetone−H_2O (1:1:1), 23 °C, 12 h, 91%; (d) (1) Ph_3SnH, Et_3B, PhMe, 23 °C, 3 h, 88%;[74] (2) NIS, THF, 23 °C, 1 h, 89%;[75] (3) *n*-BuLi, THF, −78 °C, 10 min, 63%;[76] (e) OsO_4, NMO, *t*-BuOH−acetone−H_2O (1:1:1), 23 °C, 4 days, 96%; (f) H_2, $Pd(OH)_2$ on C (cat.), MeOH, 23 °C, 12 h, 100%.

empirical rule, their stereochemistry was tentatively assigned as indicated.

Although the empirical rule is very reliable for predicting the stereochemical outcome of the osmylation of allylic alcohols and their derivatives,[37] it was desirable to have further experimental support. Thus, the two diastereomers **102** and **103** were converted into the six-membered ketols **104** and **105**, respectively (Scheme 14). The vicinal coupling constants observed for the C.37 and C.38 protons indeed verified the stereochemical assignment based on the empirical rule.

Following exactly the same sequence of reactions summarized in Scheme 13 but with the enantiomeric lactone **86**, the remaining four diastereomers **108**, **109**, **111**, and **112** were obtained, and their stereochemistry was assigned as indicated (Scheme 15).

The C.40 alcohol of MTX exists as a sulfate, which must affect the NMR characteristics of the protons and carbons in this region of the molecule. However, the degree of the effects, particularly on the protons and carbons at C.35 through C.38, may be so small that some meaningful information is expected to be gained in comparison of the NMR characteristics of the eight diastereomeric polyols **72**−**79** derived from these diastereomers with those of MTX. Thus, all of the eight diastereomers were deprotected and then subjected to the ^1H and ^{13}C NMR studies. The NMR characteristics observed for the C.34 through C.39 protons and carbons of each diastereomer were compared with those of the corresponding protons and carbons of MTX (Charts 7 and 8). This exercise indeed demonstrated that (1) the diastereomer **78** was the best match with the relevant portion of the natural product and (2) the diastereomer **75** was not as good as **78** but close. It is interesting to note that **78** and **75**

Scheme 14[a]

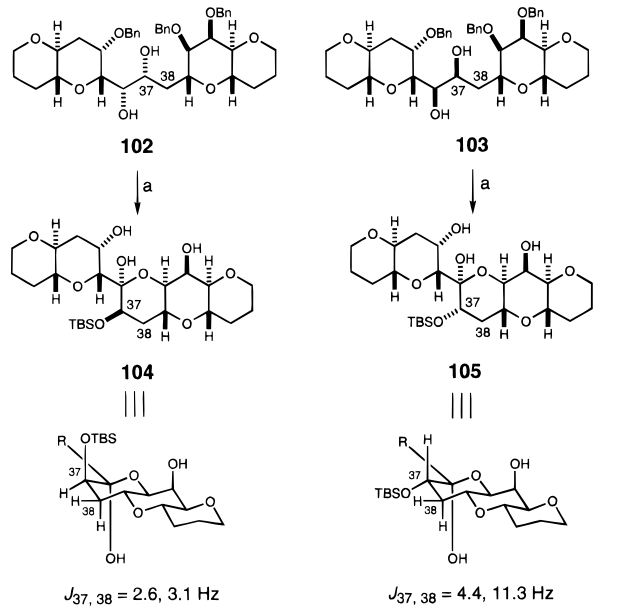

[a] (a) (1) TBSOTf, Et_3N, CH_2Cl_2, 23 °C, 68%; (2) $(COCl)_2$, DMSO, Et_3N, CH_2Cl_2, −78 °C, 99%; (3) H_2, $Pd(OH)_2$ on C (cat.), EtOAc, 23 °C, 0.5 h, 98%.

Scheme 15[a]

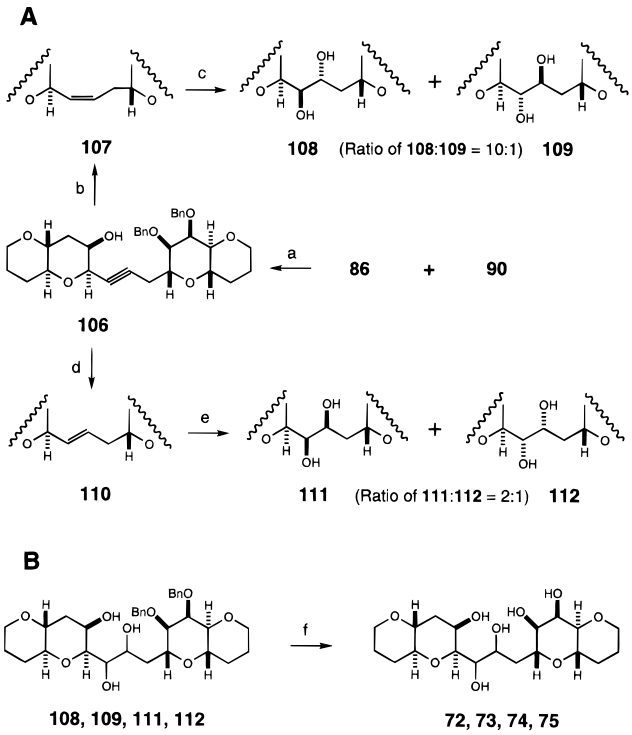

[a] Follow steps a−f of Scheme 13.

were diastereomers with respect to the C.35 and C.39 positions.[29] On the basis of these experiments, we were confident in concluding that the stereochemistry of **78** represents the stereochemistry of the corresponding part of MTX. Nevertheless, further experimental support to verify this conclusion would be desirable, and we decided to examine the spectroscopic properties of the C.40 sulfates corresponding to the **78** and **75** diastereomers.

Scheme 16 summarizes the synthesis of the C.40 sulfates **80** and **81** from **112** and **102**, respectively. The key feature in this transformation was the regiospecific reductive cleavage of the C.40−C.41 benzylidene group with DIBAL,[35] to yield exclu-

Chart 7. Difference in Proton Chemical Shifts between MTX and Each of **72**−**79** (500 MHz, 1:1 C_5D_5N−CD_3OD)

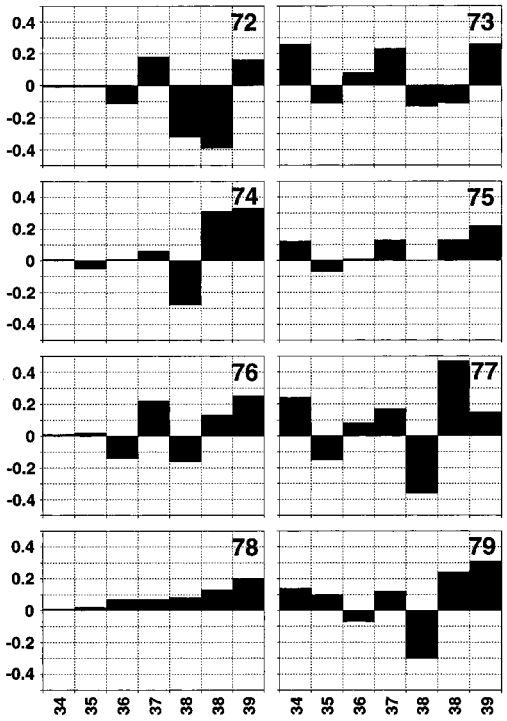

Chart 8. Difference in Carbon Chemical Shifts between MTX and Each of **72**−**79** (125 MHz, 1:1 C_5D_5N−CD_3OD)

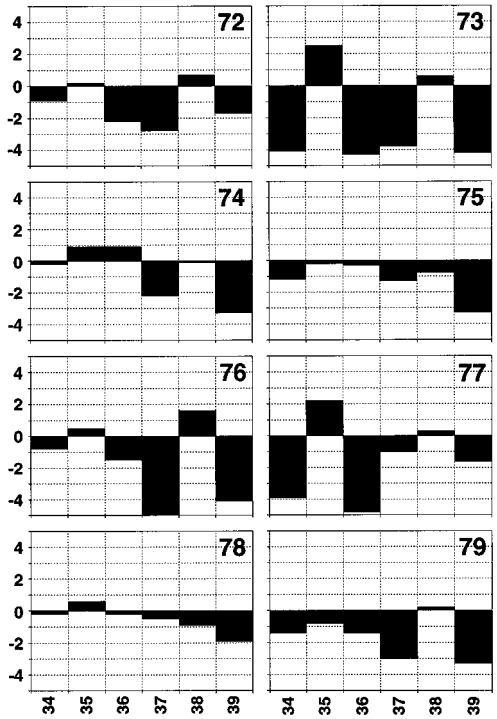

sively the C.40 alcohol **114**. The sulfates **80** and **81** were isolated as their sodium salts and then subjected to NMR studies.

Chart 9 shows the ^1H and ^{13}C NMR characteristics in the C.34−C.40 region of these diastereomers in comparison with MTX, clearly supporting the previous conclusion that the C.35 through C.39 stereochemistry of **81**, corresponding to **78**, represents the relative stereochemistry of the C.35−C.39 portion of MTX.

3. C.63−C.68 Acyclic Portion. The relative stereochemical assignment of the C.63−C.68 portion was addressed with the same approach as the one used for the C.35−C.39 portion. We chose model **F**, which possessed the relevant chiral centers at C.63, C.64, C.66, and C.68. This strategy required the synthesis of all eight possible diastereomers and the comparison of their NMR characteristics with those of the natural product.[39]

Scheme 16[a]

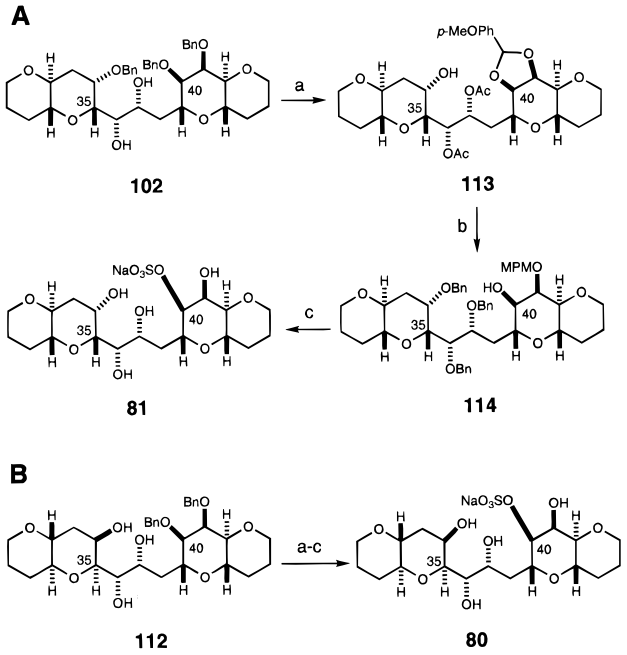

[a] (a) (1) Ac_2O, pyr, 65 °C, 2 h, 92%; (2) H_2, $Pd(OH)_2$ on C (cat.), EtOAc, 23 °C, 5 h, 100%; (3) DDQ, *p*-$MeOPhCH_2OMe$, CH_2Cl_2, 23 °C, 2 h, 93%; (b) (1) MeONa, MeOH, 23 °C, 1.5 h, 95%; (2) NaH, BnBr, THF−DMF (3:1), 23 °C, 3 h, 95%; (3) DIBAL, CH_2Cl_2, −78 °C, 5 min, then 0 °C, 20 min, 85%; (c) (1) SO_3·pyr, pyr, 23 °C, 12 h, 84%; (2) H_2, $Pd(OH)_2$ on C, MeOH, 23 °C, 12 h, 100%.

Chart 9. Difference in Proton (500 MHz, 1:1 C_5D_5N−CD_3OD) and Carbon (125 MHz, 1:1 C_5D_5N−CD_3OD) Chemical Shifts between MTX and Each of **80** and **81**

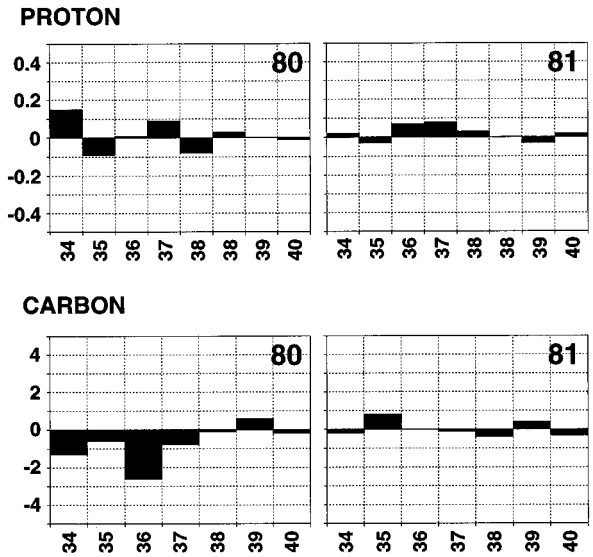

(39) Tachibana and co-workers recently reported the relative stereochemistry of the C.63−C.68 portion of MTX.[9] They opted to synthesize the four diastereomers sharing the same relative stereochemistry at the C.63 and C.64 positions. They relied on the NMR experiments in order to exclude the diastereomers bearing the opposite relative stereochemistry at the C.63 and C.64 positions. It is interesting to note that **140** and **141** were the C.68 and C.66 diastereomers of **117**, respectively.

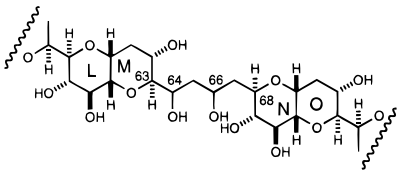

C.63-C.68 partial structure of MTX

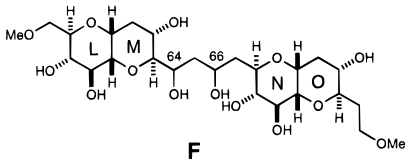

F

Scheme 17 outlines a synthetic plan for all eight diastereomers. The 1,3-diol group in **115**−**118** may be introduced via reduction of β-hydroxy ketones **119**. The β-hydroxy ketones **119** could be obtained via a 1,3-dipolar cycloaddition process, i.e., **121** + **122** → **120** → **119**, and the proposed 1,3-dipolar cycloaddition was expected to yield the two possible C.64 diastereomers. Both the olefin and the nitrile oxide required for the cycloaddition reaction could be obtained from a common intermediate **123**. The four diastereomers **115**−**118** should be secured by these experiments, and the remaining four diastereomers **138**−**141** (Scheme 21) should be available by repeating the same sequence of synthesis with the antipode of **121**.

Interestingly, we noticed that the common intermediate **123** shares its structural feature with that found in the C.28−C.37 portion of halichondrins, suggesting that its ring system could

Scheme 17

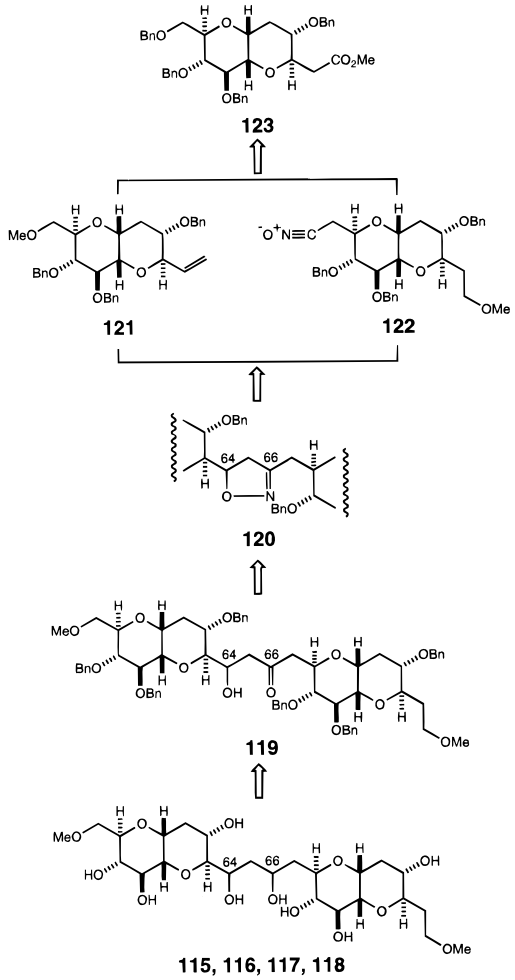

123

121 **122**

120

119

115, 116, 117, 118

Scheme 18[a]

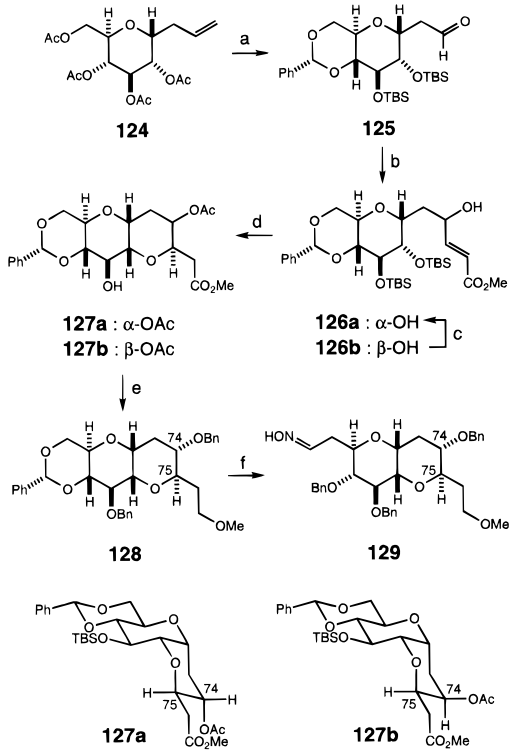

124 **125** **127a** : α-OAc **127b** : β-OAc **126a** : α-OH **126b** : β-OH **128** **129**

127a **127b**

[a] (a) (1) K_2CO_3, MeOH, 23 °C, 12 h; (2) $PhCH(OCH_3)_2$, CSA, DMF, 50 °C, 2 h; 81% over two steps; (3) TBSCl, $AgNO_3$, pyr, DMF, 23 °C, 4 h, 90%; (4) OsO_4, NMO, *t*-BuOH−THF−H_2O (3:1:1); (5) $NaIO_4$, MeOH; 80% over two steps; (b) (*E*)-ICH═$CHCO_2CH_3$, 1% $NiCl_2$/$CrCl_2$, THF-DMSO (trace), 23 °C, ratio of **126a**:**126b** = 2.5:1, 80%; (c) (1) *p*-nitrobenzoic acid, DEAD, Ph_3P, Et_2O−PhMe (2:1), 23 °C; (2) K_2CO_3, MeOH, 86% over two steps; (d) (1) Ac_2O, pyr, 91%; (2) *n*-Bu_4NF−imidazole (4:1), THF; (3) DBU, CH_2Cl_2; 77% over two steps; (e) (1) TBSOTf, *i*-Pr_2NEt, CH_2Cl_2, 83%; (2) DIBAL, Et_2O, −78 °C, 10 min, 23 °C, 1 h, 90%; (3) DMTrCl, pyr, DMAP, DMF, 0 °C, 10 min, 23 °C, 3 h; TBSCl, $AgNO_3$, pyr, DMF; PPTS, MeOH, CH_2Cl_2; 88%, three steps; (4) CH_3I, NaH, THF, 23 °C, 89%; (5) *n*-Bu_4NF, THF, 23 °C, 12 h; (6) BnBr, *n*-Bu_4NI (cat.), NaH, DMF, 23 °C, 24 h; 82% over two steps; (f) (1) DIBAL, CH_2Cl_2, −78 °C, 30 min, 23 °C, 12 h, 83%; (2) I_2, Ph_3P, imidazole, PhH, 23 °C, 1 h; (3) *n*-Bu_4NCN, DMF, 55 °C, 4 h; 82% over two steps; (4) DIBAL, PhMe, −78 °C, 2 h, then 1 N HCl, 23 °C, 2 h; (5) H_2NOH·HCl, NaOAc, EtOH, 23 °C, 1 h; 76% over two steps.

be constructed by adopting the method developed for the synthesis of halichondrins.[40] Indeed, this was effectively carried out (Scheme 18). The axial *C*-allylglucose tetraacetate **124**[41] was used as the starting material, and the C.74−C.75 bond was formed via the Ni(II)/Cr(II)-mediated coupling[42] of the aldehyde **125** with methyl *(E)*-β-iodoacrylate, to yield a 5:2 mixture of two possible diastereomers. These diastereomers were interconvertible via the Mitsunobu reaction.[43] On the basis of the previous examples,[40] the stereochemistry of the major product was tentatively assigned. The bicyclic ring system was stereospecifically constructed via the Michael reaction.[44] The ^1H NMR analysis of the Michael adduct acetates **127a,b**, derived

(40) (a) Aicher, T. D.; Buszek, K. R.; Fang, F. G.; Forsyth, C. J.; Jung, S. H.; Kishi, Y.; Scola, P. M. *Tetrahedron Lett.* **1992**, *33*, 1549−1552. (b) Aicher, T. D.; Buszek, K. R.; Fang, F. G.; Forsyth, C. J.; Jung, S. H.; Kishi, Y.; Matelich, M. C.; Scola, P. M.; Spero, D. M.; Yoon, S. K. *J. Am. Chem. Soc.* **1992**, *114*, 3162−3164 and references cited therein.

(41) Giannis, A.; Sandhoff, K. *Tetrahedron Lett.* **1985**, *26*, 1479−1482.

(42) (a) Jin, H.; Uenishi, J.-i.; Christ, W. J.; Kishi, Y. *J. Am. Chem. Soc.* **1986**, *108*, 5644−5646. (b) Takai, K.; Kimura, K.; Kuroda, T.; Hiyama, T.; Nozaki, H. *Tetrahedron Lett.* **1983**, *24*, 5281−5284.

(43) Mitsunobu, O. *Synthesis* **1981**, 1−28.

(44) Protection of the allylic hydroxy group was necessary to have a clean and efficient cyclization.

Scheme 19[a]

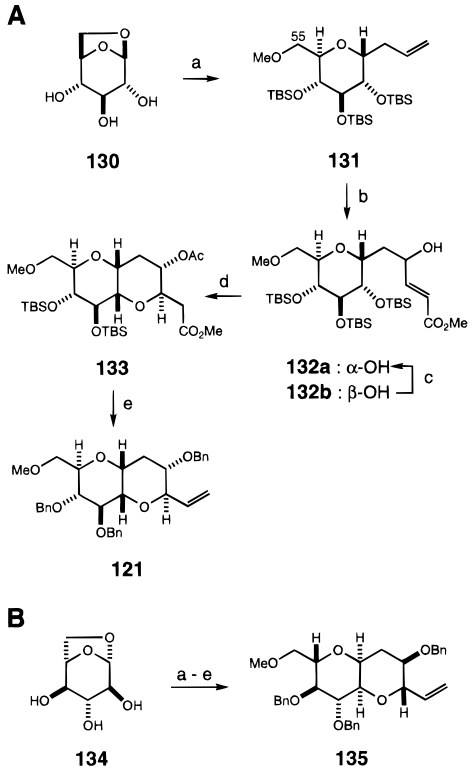

[a] (a) (1) Benzylation and silylallylation, see ref 31; (2) MeI, NaH, THF, 23 °C; (3) Na, NH_3, THF, −78 °C; (4) TBSOTf, *i*-Pr_2NEt, CH_2Cl_2, 23 °C; (b) (1) O_3, CH_2Cl_2−MeOH (3:1), −78 °C; Ph_3P, 98%; (2) (*E*)-ICH=$CHCO_2CH_3$, 1% $NiCl_2/CrCl_2$, THF, 23 °C, ratio of **132a**:**132b** = 1:1, 90%; (c) (1) *p*-nitrobenzoic acid, DEAD, Ph_3P, PhMe, 23 °C, 4 h; (2) K_2CO_3, MeOH, 99%; (d) (1) Ac_2O, pyr; (2) HF·pyr, CH_3CN, 0 °C, 4 h, 67%; (3) DBU, CH_2Cl_2, 20 h, 81%; (4) TBSCl, $AgNO_3$, imidazole, DMF, 89%; (e) (1) DIBAL, Et_2O, −78 °C, 10 min, 23 °C, 1 h, 95%; (2) PvCl, pyr, 0 °C, 92%; TBSCl, imidazole, DMF, 23 °C, 2 h; DIBAL, Et_2O, −78 °C, then 10 min, 23 °C, 1 h, 100% over two steps; (3) I_2, Ph_3P, imidazole, PhH, 95%; $(PhSe)_2$, $NaBH_4$, EtOH, 23 °C; $NaIO_4$;[77] *i*-Pr_2NH, 81% over two steps; (4) *n*-Bu_4NF, THF; BnBr, *n*-Bu_4NI (cat.), NaH, DMF, 23 °C, 24 h, 91% over two steps.

Scheme 20[a]

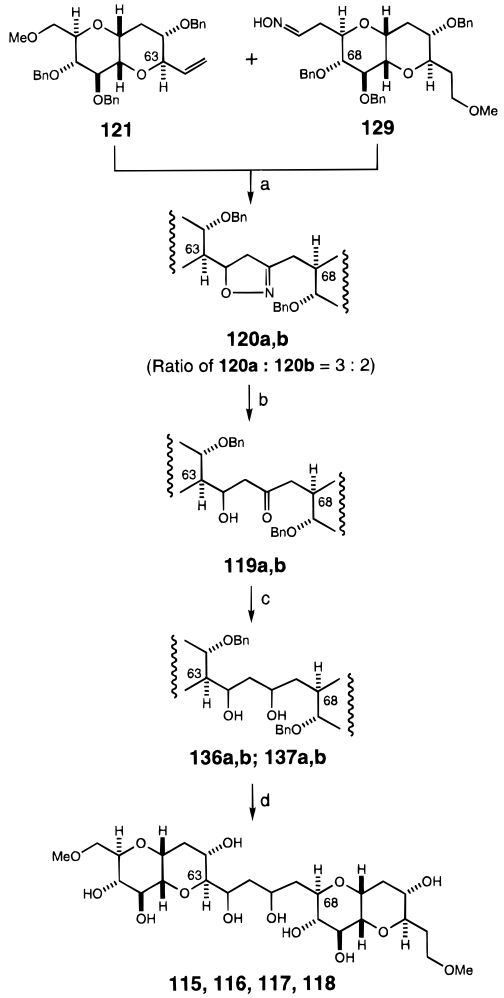

[a] (a) (1) NCS, $CHCl_3$, pyr (trace), 23 °C, 1 h; (2) **121**, *i*-Pr_2NEt, $CHCl_3$, 0 °C, 15 min, then 60 °C, 24 h; 50−60%; (b) $Mo(CO)_6$, CH_3CN-H_2O (8:1), 80 °C, 70−80%; (c) $NaBH(OAc)_3$, AcOH−CH_3CN (1:1), 23 °C, 10 h, 80−90%; (d) $Pd(OH)_2$ on C (cat.), H_2 (1 atm), MeOH−EtOAc (1:1), 90%.

from the major and minor diastereomers **126a,b** obtained in the Ni(II)/Cr(II)-mediated coupling reaction, confirmed the tentative stereochemical assignment; most critically, the coupling constant between the C.74-H and C.75-H was found to be 10 Hz for **127a**, whereas it was approximately 2 Hz for **127b**. With this evidence for the stereochemical assignment, the major Michael product **127a** was then transformed into the aldoxime **129**.

As pointed out, the olefin partner **121** for the 1,3-dipolar cycloaddition could be prepared from some intermediates in Scheme 18. For technical reasons, however, it was decided that the C.55 alcohol should be converted to its methyl ether at the very beginning of the synthesis. Thus, using the same chemistry as the one shown in Scheme 18, the axial *C*-allylglucoside derivative **131**, readily available from 1,6-anhydro-D-glucose (**130**),[31,45] was converted into the olefin **121** (Scheme 19A). Similarly, its antipode **135** was obtained from 1,6-anhydro-L-glucose (**134**; Scheme 19B).[46]

The 1,3-dipolar cycloaddition between **121** and **129** took place smoothly at 60 °C, to yield a 3:2 mixture of the expected adducts **120a,b** in 50−60% combined yield.[47,48] The two adducts were separated by silica gel column chromatography and then subjected to the three-step sequence of transformation, i.e., (1) reductive cleavage of the N−O bond with molybdenum hexacarbonyl,[49] to yield *β*-hydroxy ketones **119a,b**; (2) reduction of the resultant *β*-hydroxy ketone **119a** with sodium triacetoxyborohydride,[50] to give a ca. 4:1 ratio of the two possible diols, which were separated by silica gel column chromatography; and (3) deprotection of the benzyl groups, to furnish the polyols **115** and **116**. From the second cycloaddition product **119b**, the third and fourth polyols **117** and **118** were similarly obtained (Scheme 20). Exactly the same chemistry was applied for the olefin **135** derived from 1,6-anhydro-L-glucose (**134**), to furnish the remaining four diastereomers **138**−**141** (Scheme 21).

All of the eight diastereomers were then subjected to the ^1H and ^{13}C NMR study, and the chemical shifts observed for the C.62 through C.69 protons and carbons of each diastereomer were compared with those corresponding to MTX (Charts 10

(45) Coleman, G. H. In *Methods in Carbohydrate Chemistry*; Whistler, R. L., Wolfrom, M. L., Eds.; Academic Press: New York and London, 1963; Vol. II, pp 397−399.

(46) **134** was prepared from commercially available L-glucose.[45]

(47) With TBS groups as the hydroxy protecting groups, the 1,3-dipolar cycloaddition failed to give acceptable yields. Change of the TBS groups into benzyl groups resulted in improved and reproducible yields.

(48) For a review on the nitrile oxide coupling reaction, for example, see: Torssell, K. B. G. *Nitrile Oxides, Nitrones, and Nitronates in Organic Synthesis*; VCH: New York; 1987; Chapter 2.

(49) Baraldi, P. G.; Barco, A.; Benetti, S.; Manfredini, S.; Simoni, D. *Synthesis* **1987**, 276−278.

(50) Evans, D. A.; Chapman, K. T.; Carreira, E. M. *J. Am. Chem. Soc.* **1988**, *110*, 3560−3578.

Scheme 21[a]

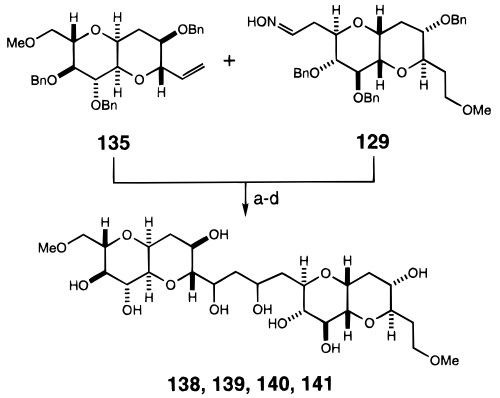

[a] Follow steps a−d of Scheme 20.

Chart 10. Difference in Proton Chemical Shifts between MTX and Each of **115**−**118** and **138**−**141** (500 MHz, 1:1 C_5D_5N−CD_3OD)

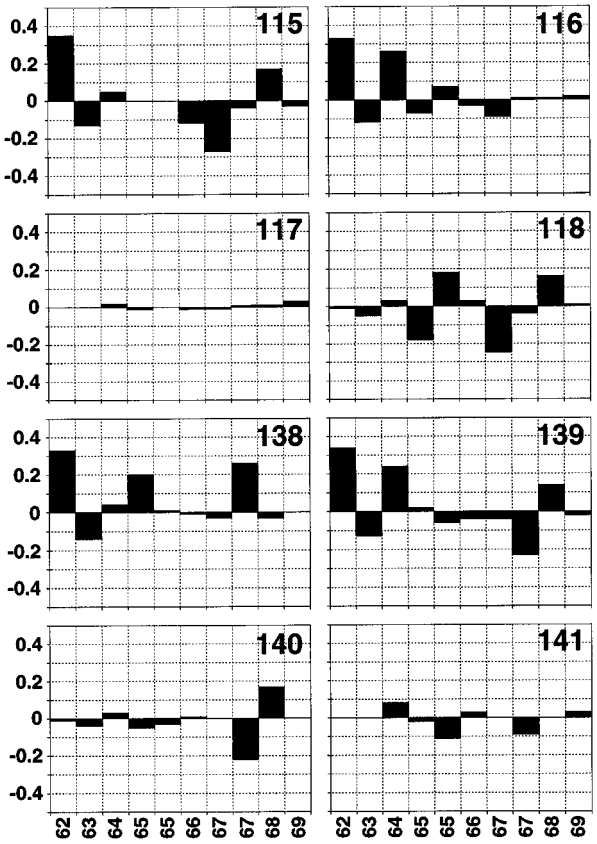

and 11). This exercise clearly demonstrated that (1) each diastereomer exhibited distinct spectroscopic characteristics differing from the others and (2) only the diastereomer **117** displayed NMR characteristics that were virtually identical to those of this portion of MTX.

Having demonstrated that the diastereomer **117** represents the relative stereochemistry of this portion of MTX, we then established its stereochemistry from the following experiments. Since the diastereomer **117** originated from the cycloaddition product between **121** and **129**, the stereochemistry at the C.63 and C.68 positions was firmly known, but the stereochemistry at the C.64 and C.66 positions was not established at this stage. In order to establish the C.64 stereochemistry, the diastereomers **119a**,**b** were transformed into the cyclic hemiketal peracetates **142a**,**b**, respectively (Scheme 22). The C.64 proton signal was observed as a doublet of doublets of doublets (J = 11.3, 9.5,

Chart 11. Difference in Carbon Chemical Shifts between MTX and Each of **115**−**118** and **138**−**141** (125 MHz, 1:1 C_5D_5N−CD_3OD)

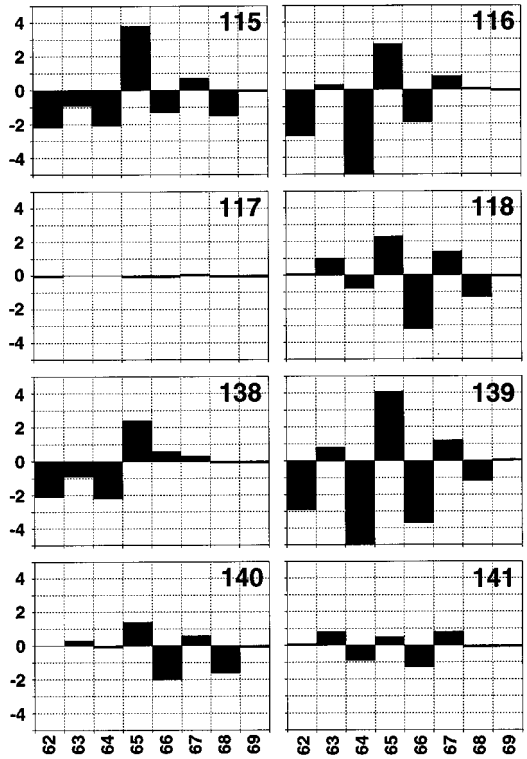

Scheme 22[a]

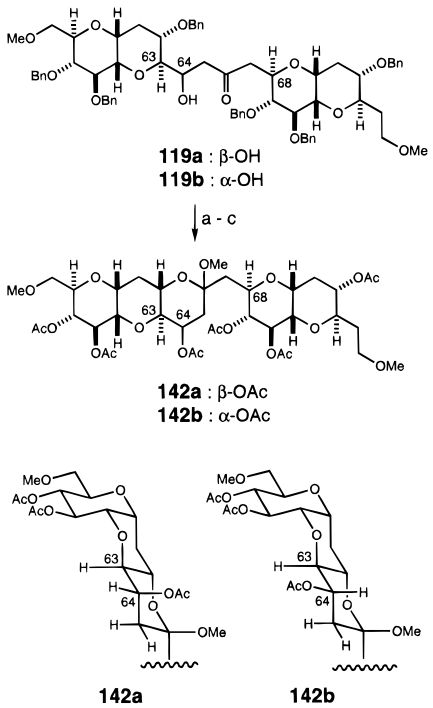

[a] (a) H_2, $Pd(OH)_2$ on C (cat.), EtOAc−MeOH (1:1); (b) $CHCl_3$−MeOH (5:1), PPTS, 23 °C; (c) Ac_2O, pyr.

and 5.3 Hz) at 5.56 ppm for the isomer **142b**, derived from **119b**, whereas a broad doublet of doublets was observed (J = 5.5 and 2.6 Hz) at 5.39 ppm for the isomer **142a**, derived from **119a**. Coupled with the fact that the newly formed six-membered ring clearly adopted a chair conformation (for example, $J_{62,63}$ = 9.8 Hz for **142a** and $J_{62,63}$ = 9.6 Hz for **142b**), the values of these vicinal coupling constants established the C.64 stereochemistry of **117** as depicted in Scheme 23.

Scheme 23[a]

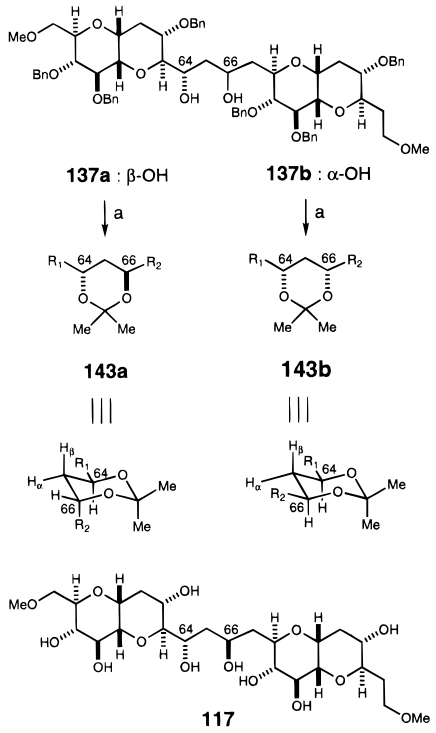

[a] (a) $MeC(OMe)_2Me$, PPTS, CH_2Cl_2, 23 °C.

The relative stereochemistry between C.64 and C.66 was then determined from the following experiments. Both the diols **137a,b**, obtained from the reduction of the β-hydroxy ketone **119b** with sodium triacetoxyborohydride, were converted into the acetonides **143a,b** (Scheme 23). The vicinal coupling constants $J_{64,65(\beta)} = 9.8$ Hz and $J_{65(\beta),66} = 6.1$ Hz were observed for the acetonide **143a** derived from **137a**, whereas the constants $J_{64,65(\beta)} = J_{65(\beta),66} = 12.0$ Hz were observed for the acetonide **143b** derived from **137b**. These vicinal proton coupling constants confirmed the stereochemistry at C.64 and C.66, thereby establishing that **117** (Scheme 23) represents the relative stereochemistry of this acyclic portion of MTX.

4. C.134−C.142 Acyclic Portion. The C.134−C.142 portion of MTX contained five chiral centers in question, giving rise to 16 possible diastereomers. We decided to adopt the same approach as the one used for the C.35−C.39 and the C.63−C.68 portions, and we chose **G** as the model for this purpose. The angular methyl substituents were substituted by hydrogens to simplify the synthesis with the belief that this substitution would not greatly alter the structural characteristics of the acyclic chain.

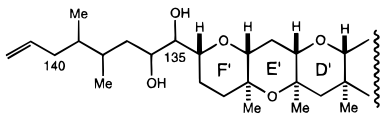

C.134-C.142 partial structure of MTX

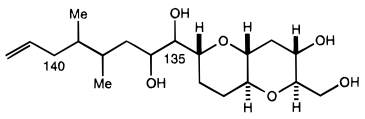

G

Scheme 24 outlines a synthetic plan for all 16 diastereomers. The proposed synthesis is convergent, in which the problem of preparing these diastereomers was first reduced to the preparation of four acetylene intermediates. For example, the coupling

Scheme 24

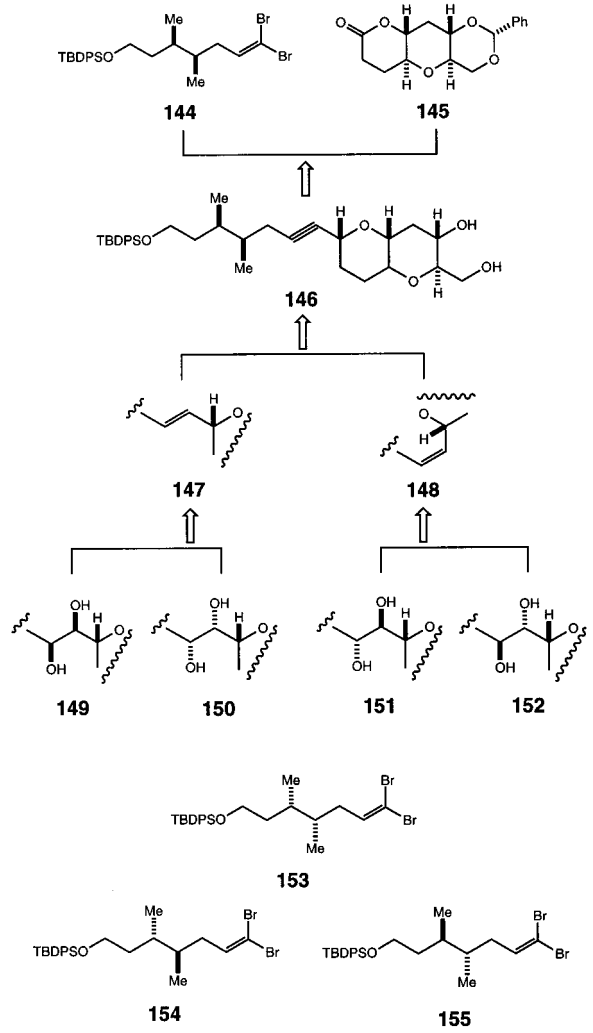

of the acetylene anion generated from the dibromo olefin **144** with the lactone **145**, followed by silane reduction, is expected to yield stereoselectively the equatorial acetylene **146**, which could, in turn, be reduced to either the *trans*- or *cis*-olefin **147** or **148**. Osmylation of these olefins should give the four diols **149**−**152**. Application of this synthesis to the remaining three acetylene equivalents **153**−**155** should result in the remaining 12 diastereomeric diols.

The synthesis of the lactone **145** began with methyl D-glucopyranoside derivative **156**[51] (Scheme 25). The C.129 alcohol was removed under the Barton conditions, and the equatorial *C*-glycosidation was stereoselectively accomplished by addition of allylmagnesium bromide to the lactone **157**, followed by silane reduction.

Scheme 26 summarizes the synthesis of *anti*- and *syn*-dimethyl dibromo olefins **161** and **164**. The relative stereochemistry of the C.138 and C.139 methyl groups was set by the Diels−Alder reaction. It should be noted that these syntheses were purposely carried out in a racemic form so that all of the four required diastereomers of dibromo olefins were obtained in only two syntheses.

The anion, generated from the racemic *anti*-dimethyl dibromo olefin **161**, was coupled with the lactone **145**, followed by triethylsilane reduction in the presence of $BF_3{\cdot}Et_2O$. The NMR spectra of the crude reaction mixture showed no detectable amount of the axial products, but the two equatorial *anti*-

(51) Koto, S.; Takebe, Y.; Zen, S. *Bull. Chem. Soc. Jpn.* **1972**, *45*, 291−293.

Scheme 25[a]

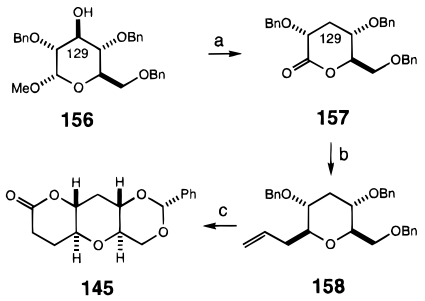

[a] (a) (1) (i) NaH, CS_2, MeI, THF, 23 °C; (ii) Bu_3SnH, AIBN, PhMe, 110 °C; 90% over two steps; (2) 1N HCl, AcOH, 60 °C, 70%; (3) $(COCl)_2$, DMSO, Et_3N, CH_2Cl_2, −78 °C, 60%; (b) (1) allylmagnesium bromide, THF, −78 °C; (2) Et_3SiH, $BF_3{\cdot}OEt_2$, CH_2Cl_2, −20 °C; 55% over two steps; (c) (1) (i) catecholborane, $(PPh_3)_3RhCl$, THF, 23 °C; (ii) 30% H_2O_2, 3 N NaOH, 23 °C, 90% over two steps; (2) Jones oxidation, 80%; (3) H_2, $Pd(OH)_2$ on C, MeOH, 23 °C, 85%; (4) $PhCH(OMe)_2$, *p*-TsOH, DMF, in vacuum at 50 °C, 90%; (5) CSA, PhH, 80 °C, 95%.

Scheme 26[a]

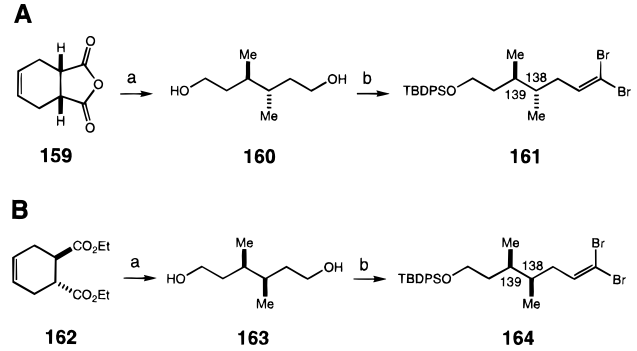

[a] (a) (1) LAH, THF, 23 °C, 85%; (2) *p*-TsCl, pyr, 23 °C, 90%;[78] (3) (i) LAH, THF, 65 °C; (ii) O_3, CH_2Cl_2, −78 °C; (iii) $NaBH_4$, THF−CH_2Cl_2−MeOH, 23 °C, 30% over three steps; (b) (1) TBDPSCl, pyr, DMF, 23 °C, 33%; (2) $(COCl)_2$, DMSO, Et_3N, CH_2Cl_2, −78 °C, 80%; (3) PPh_3, CBr_4, 0 °C, 95%.

Scheme 27[a]

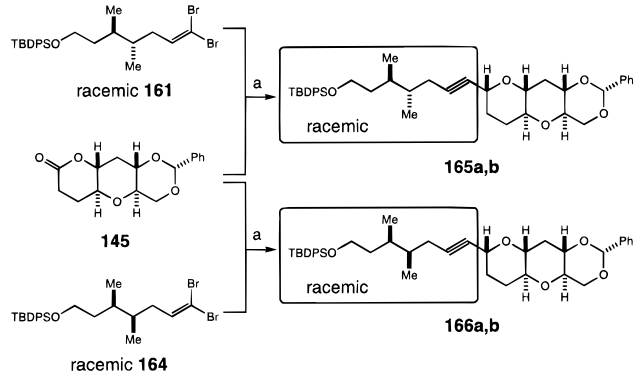

[a] (a) (1) *n*-BuLi, THF, −78 °C; (2) Et_3SiH, $BF_3{\cdot}OEt_2$, CH_2Cl_2, −25 °C; 70% over two steps.

dimethyl acetylenes **165a,b** were chromatographically inseparable at this stage. Similarly, the combination of **145** and **164** furnished exclusively the two equatorial *syn*-dimethyl acetylenes **166a,b** as an inseparable mixture (Scheme 27).

The *anti*-dimethyl acetylene mixture **165a,b** was converted into the *trans*-olefins **167a,b** in three steps, which were then subjected to osmylation, to furnish the four possible *threo* diols **168**−**171**. Fortunately, these four diastereomers were easily separable by silica gel column chromatography at this stage. The *anti*-dimethyl acetylene mixture **165a,b** was also reduced

Scheme 28[a]

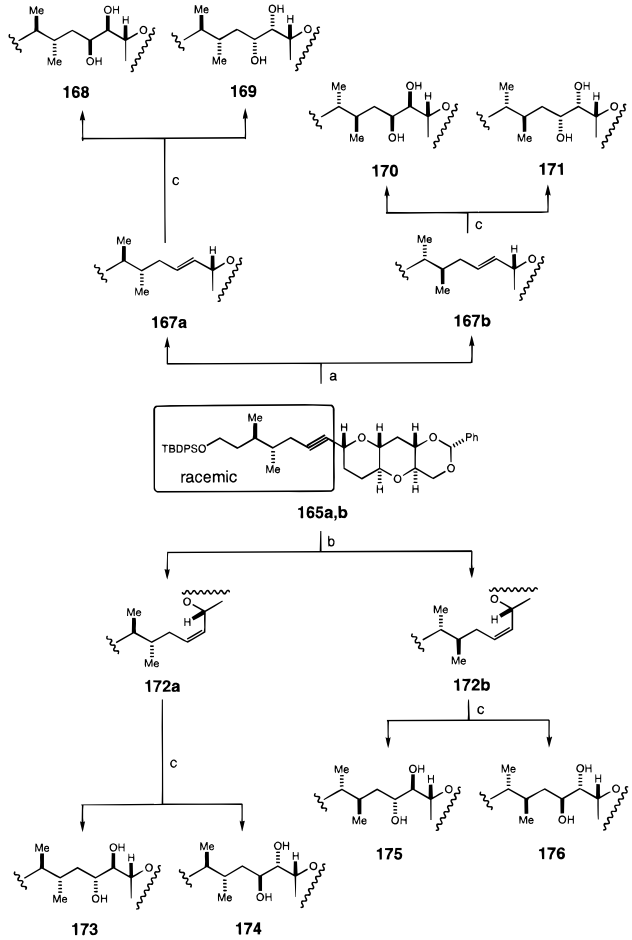

[a] (a) (1) Ph_3SnH, BEt_3, PhMe, 23 °C; (2) NIS, THF, 23 °C; (3) *n*-BuLi, THF, −78 °C, 75% over three steps; (b) H_2, Lindlar catalyst, EtOAc, 23 °C, 95%; (c) OsO_4, NMO, H_2O−acetone−*t*-BuOH (1:1:1), 23 °C, 2:1.

under Lindlar conditions to the *cis*-olefins **172a,b**, which were subjected to osmylation, followed by chromatographic separation, to furnish the four possible *erythro* diols **173**−**176** (Scheme 28).

Using the same methods, the four *threo* diols **178**−**181** and the four *erythro* diols **183**−**186** were obtained from the two equatorial *syn*-dimethyl acetylenes **166a,b** (Scheme 29).

These diastereomers were subjected to a sequence of reactions to furnish all of the 16 models **187**−**202** (Scheme 30). As before, their ^1H and ^{13}C NMR characteristics were examined in reference to those of the natural product (Charts 12 and 13). This exercise demonstrated that (1) each diastereomer once again exhibited distinct spectroscopic characteristics differing from those of the others; (2) only one diastereomer, **187**, exhibited spectroscopic characteristics that were virtually identical to those of the C.134−C.142 portion of MTX; and (3) this matching diastereomer was found to be one of the four possible diastereomers belonging to the *syn*-diol/*anti*-dimethyl series, i.e., the diastereomers originating from **168**−**171**.

The relative stereochemistry of the matching diastereomer was deduced from the experiments shown in Scheme 31. The methyl group at C.3 of (*S*)-citronellal (**203**) was transformed into the C.164 methyl group of **167a**, establishing the relative stereochemistry at C.134, C.138, and C.139. Osmylation of **167a** yielded a 2:1 mixture of the two possible *threo* diols, with the matching diastereomer being the minor product **187**. On the basis of the empirical rule,[37] the stereochemistry of the minor, matching diol was assigned to be **187**. This assignment

Scheme 29[a]

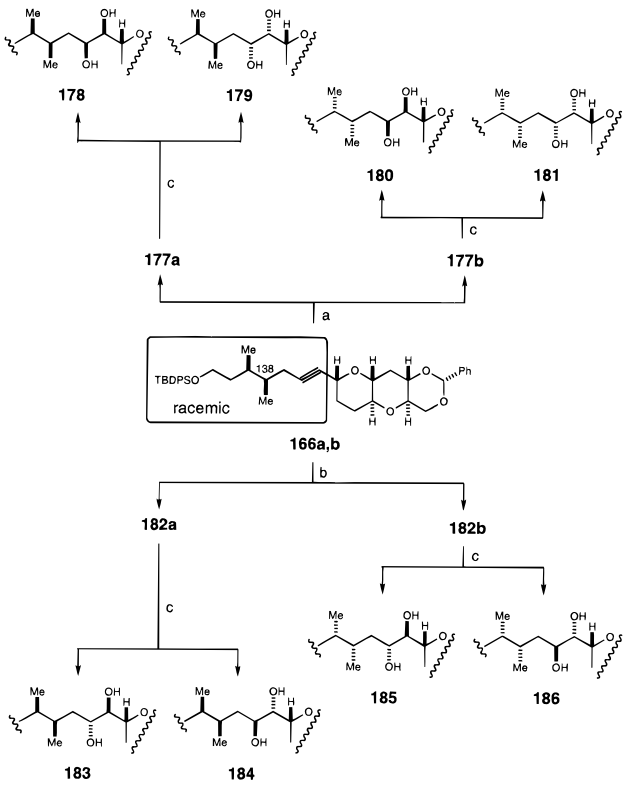

[a] The structures of **177a,b** and **182a,b** correspond to those of **167a,b** and **172a,b** in Scheme 28, respectively, except that the C.138 configuration is opposite in this series. Follow steps a−c of Scheme 28.

Scheme 30[a]

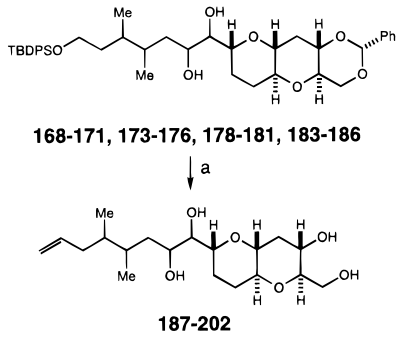

[a] (a) (1) $MeC(OMe)_2Me$, PPTS, DMF, 23 °C, 95%; (2) *n*-Bu_4NF, THF, 23 °C, 95%; (3) $(COCl)_2$, DMSO, Et_3N, CH_2Cl_2; (4) *n*-BuLi, Ph_3PCH_3Br, THF, 0 °C, 77% over two steps; (5) aqueous AcOH, 50 °C, 99%.

was further supported from the results on asymmetric osmylation using both AD-mix α and AD-mix β reagents;[52] the diol **187** was formed as the major product with AD-mix α, whereas the diol **188** was the exclusive product with AD-mix β. These results were consistent with the principle of double stereodifferentiation,[18] i.e., the precedents known for asymmetric induction with these AD-mix reagents[52] coupled with the stereochemical outcome predicted by the empirical rule.[37] Thus, the relative stereochemistry of this diastereomer, and consequently this portion of MTX, was established as **187**.

5. Complete Relative Structure. MTX contains 32 rings, all of which exist as fused-ring systems. Using primarily the NMR methods, Yasumoto and co-workers have successfully determined the relative stereochemistry of these fused-ring

(52) For a recent review, see: Kolb, H. C.; VanNieuwenhze, M. S.; Sharpless, K. B. *Chem. Rev.* **1994**, *94*, 2483−2547.

Chart 12. Difference in Proton Chemical Shifts between MTX and Each of **187**−**202** (500 MHz, 1:1 $C_5D_5N-CD_3OD$)

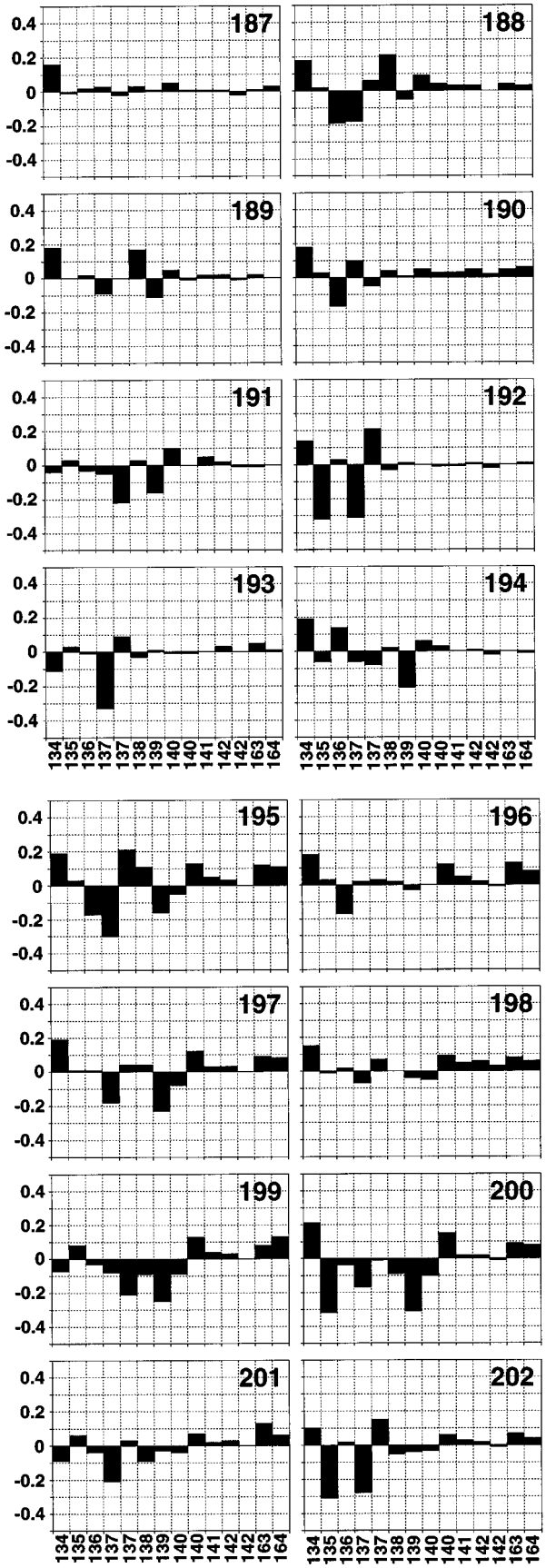

portions. At three places, the fused-polycyclic systems are connected directly via a single carbon−carbon bond, i.e., the

Chart 13. Difference in Carbon Chemical Shifts between MTX and Each of **187**−**202** (125 MHz, 1:1 C_5D_5N−CD_3OD)

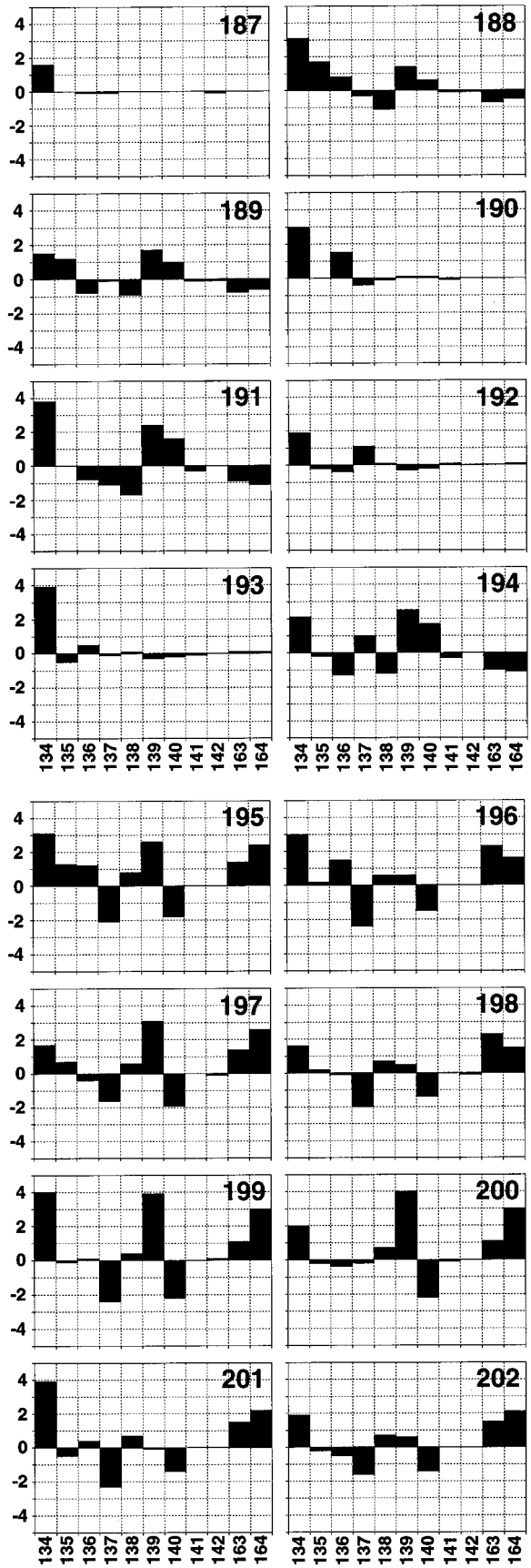

K/L-, O/P-, and V/W-ring junctures. Relying on the NOE and $^3J_{H,H}$ data with the aid of molecular mechanics calculations (MM2), they have also studied the relative stereochemistry of these ring junctures and have proposed the structure **1A** as the partial relative stereostructure of MTX.[53] Coupled with this information, the present work allows the assignment of the structure **1B** (Figure 3) as the complete relative stereochemistry of MTX.

Scheme 31[a]

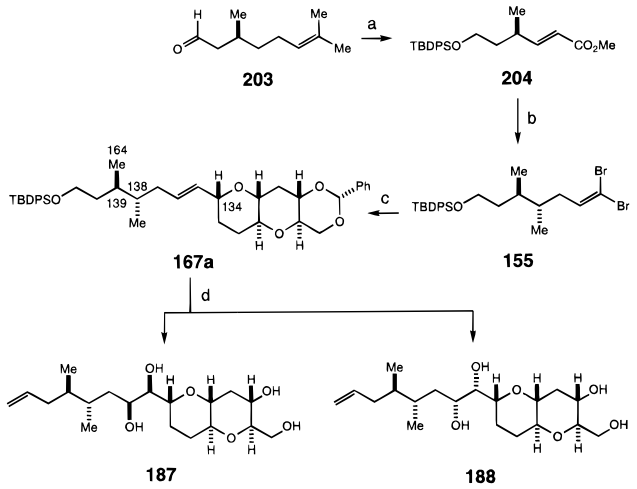

[a] (a) (1) $NaBH_4$, MeOH, 23 °C; (2) TBDPSCl, pyr, DMF, 23 °C; (3) O_3, NaOH, MeOH-CH_2Cl_2, −78 °C, 50% over three steps; (4) (i) LDA, PhSeBr, THF, −78 °C; (ii) 30% H_2O_2, CH_2Cl_2, 0 °C, 59% over two steps; (b) (1) MeLi, CuI, THF, BF_3·OEt_2, −78 °C to 0 °C (3:2 *anti*/*syn*);[79] (2) LAH, THF, 23 °C, 51% over two steps; (3) *(R)*-(−)-1-(1-naphthyl)ethyl isocyanate, Et_3N, PhMe, 60 °C, 82%; (4) LAH, THF, 50 °C, 51%; (5) $(COCl)_2$, DMSO, Et_3N, CH_2Cl_2, −78 °C, 79%; (6) PPh_3, CBr_4, 0 °C, 95%; (c) (1) *n*-BuLi, **145**, −78 °C; (2) Et_3SiH, BF_3·OEt_2, CH_2Cl_2, −25 °C; 70% over two steps; (3) Ph_3SnH, BEt_3, PhMe, 23 °C; (4) NIS, THF, 23 °C; (5) *n*-BuLi, THF, −78 °C, 70% over three steps; (d) (1) AD-mix α, H_2O−*t*-BuOMe−*t*-BuOH (1:1:1), 23 °C, 53%; (2) $MeC(OMe)_2Me$, PPTS, DMF, 23 °C, 90%; (3) *n*-Bu_4NF, THF, 23 °C, 95%; (4) $(COCl)_2$, DMSO, Et_3N, CH_2Cl_2, −78 °C; (5) *n*-BuLi, Ph_3PCH_3Br, THF, 0 °C, 77% over two steps; (6) aqueous TFA−MeOH−H_2O (1:1:1), 50 °C, 99%.

(53) The relative stereochemistry of the K/L- and O/P-ring junctures has been determined on the basis of the NOE and $^3J_{H,H}$ data with the aid of molecular mechanics calculations (MM2). However, the presence of the C.155 methyl group precludes the use of the $^3J_{H,H}$ data between the ring-juncture protons for elucidating the relative stereochemistry at C.99−C.100. Thus, their conclusion on the relative stereochemistry of the V/W-ring juncture was less sound than that on the O/P- and V/W-ring junctures. The experimental data given in ref 6c and its supplementary material do not necessarily exclude the alternative relative stereochemistry, cf. the partial structure **x**. In principle, the two possible stereostructures **ix** and **x** should be distinguishable from the patterns of the NOE connectivity among the protons at C.98(α), C.98(*β*), C.99, C.101, and C.155. However, because of many overlapping peaks present in the spectrum given in the supplementary material, this distinction was not obvious. It should be noted that the relative stereochemistry of the alternative possibility **x** coincides with that of the K/L- and O/P-ring junctures. If the alternative possibility is the case, the stereochemistry of MTX is represented by the structure bearing the opposite relative stereochemistry at C.5 through C.99 of **1B** and **1C**.

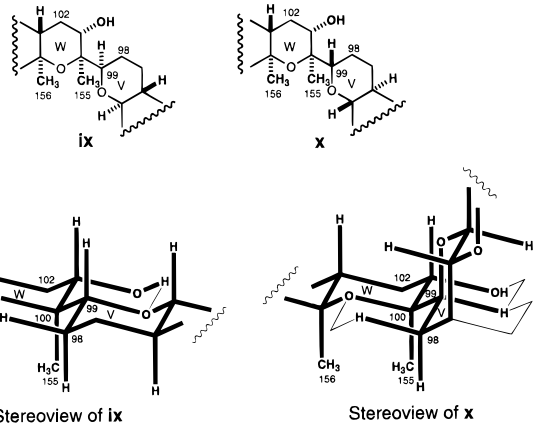

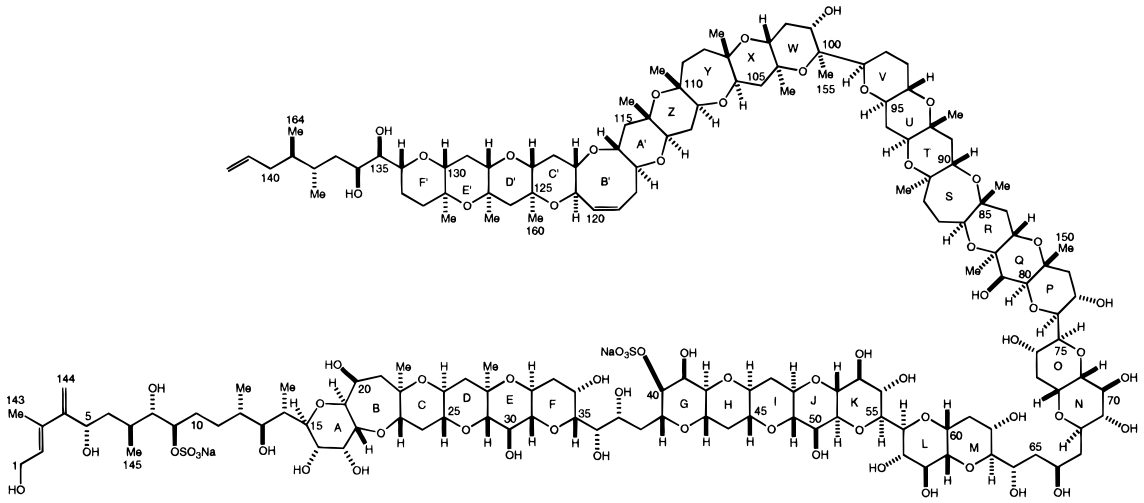

Figure 3. 1B: Complete relative structure of maitotoxin.

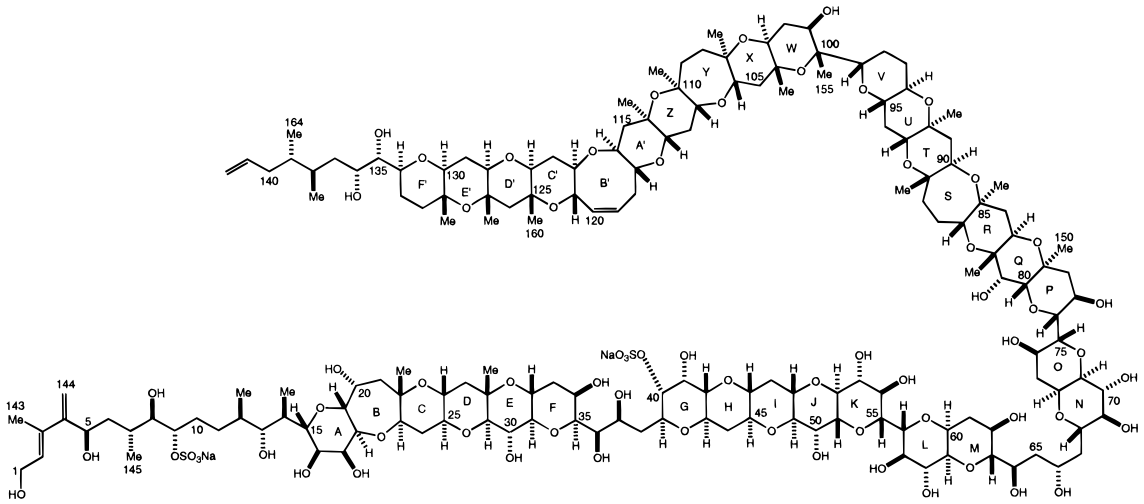

Figure 4. 1C.

III. Absolute Stereochemistry

Obviously, MTX is structurally similar to brevetoxins, ciguatoxins, and related marine natural products.[1a] It is likely that these natural products share the same absolute configuration.[54] On this assumption, the absolute stereochemistry of MTX may be suggested, but there are two obstacles to consider. First, among these natural products, brevetoxin B (**205**) is the only member whose absolute stereochemistry has been definitively established.[55] Second, the structural correlation of brevetoxin B and MTX is not trivial, particularly assigning, in a biogenetic sense, the head and tail to these natural products. However, focusing on the structural resemblance between the ring E′−Y portion of MTX to the ring K−D portion of brevetoxin B, one may suggest that the absolute configuration of MTX is more likely **1B**. However, the work by Hirama, Yasumoto, and co-workers should also be noted. On the basis of the CD spectrum of the synthetic AB ring model, they suggested the absolute configuration of gambiertoxin 4B (**206**) and ciguatoxin.[56,57] That suggested absolute configuration of gambiertoxin 4B/ciguatoxin matches that of brevetoxin B, assuming that the C.1−ring A moiety of gambiertoxin 4B/ciguatoxin and the C.42−ring K moiety of brevetoxin B represent the head (or tail) in a biogenetic sense. The biogenetic structural correlation of MTX with gambiertoxin 4B/ciguatoxin is less obscure than that with brevetoxin B; focusing on a vicinal dimethyl group present in both natural products, the C.142−ring F′ moiety of MTX appears to correspond to the ring M/L moiety of gambiertoxin 4B/ciguatoxin. On the basis of these considerations, the more likely absolute structure of MTX then seems to be **1C** (Figure 4), the antipode of **1B**.

IV. Preferred Solution Conformation

As noted, MTX contains 32 rings, all of which exist as fused-ring systems. Except for two, they are *trans*-fused, and they are expected to be relatively rigid conformationally, which is indeed demonstrated through the extensive NMR studies by Yasumoto and co-workers.[6] At three places, two of these fused-polycyclic portions are connected directly via a single carbon−carbon bond, i.e., the K/L-, O/P-, and V/W-ring junctures. Yasumoto and co-workers have also studied the preferred

(54) It should be noted that ciguatoxins and MTX are known to originate from *Gambierdiscus toxicus*, whereas brevetoxins are from *Gymnodinium breve*.

(55) Lin, Y.-Y.; Risk, M.; Ray, S. M.; Van Engen, D.; Clardy, J.; Golik, J.; James, J. C.; Nakanishi, K. *J. Am. Chem. Soc.* **1981**, *103*, 6773−6775. The absolute configuration of brevetoxin B was determined by using the dibenzoate chirality method on a di-*p*-bromobenzoate derivative. The recent total synthesis of brevetoxin B by Nicolaou (Nicolaou, K. C.; Rutjes, F. P. J. T.; Theodorakis, E. A.; Tiebes, J.; Sato, M.; Untersteller, E. *J. Am. Chem. Soc.* **1995**, *117*, 10252−10263) confirmed the assignment.

(56) Suzuki, T.; Sato, O.; Hirama, M.; Yamamoto, Y.; Murata, M.; Yasumoto, T.; Harada, N. *Tetrahedron Lett.* **1991**, *32*, 4505−4508.

(57) The original suggestion has recently been supported by further experiments: a private communication from Professor Masahiro Hirama at Tohoku University (March 1996).

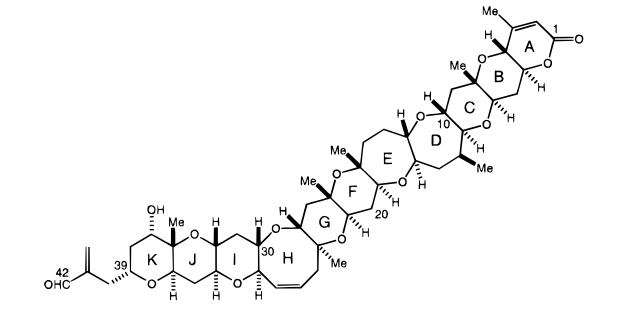

205 : Brevetoxin B

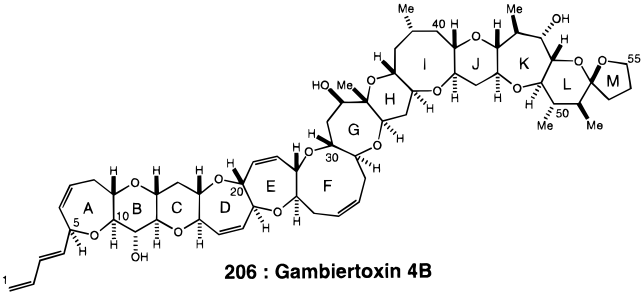

206 : Gambiertoxin 4B

conformation for these moieties by NMR methods, coupled with force-field computation. It is worth noting that the K/L- and O/P-ring systems are structurally similar to the case studied by Still,[58] and their conformational characteristics match each other well.

In order to estimate the overall conformational properties of MTX, the information regarding the remaining acyclic portions, i.e., C.1−C.15, C.35−C.39, C.63−C.68, and C.134−C.142, must be addressed. The vicinal proton coupling constants observed for models **51**, **81**, **117**, and **187** provide indispensable conformational information. It should be restated that, as the NMR characteristics observed for these models were virtually superimposable on those of the relevant protons and carbons of MTX itself, the preferred conformations found for these models should adequately represent the preferred solution conformation of MTX as well.

Figure 5 summarizes the vicinal proton spin coupling constants observed for model **187**, suggesting the preferred conformation of this portion of MTX to be represented by **187A**. Several characteristics are worth noting. First, the C.134−C.135 *C*-glycosidic bond preferentially adopts the *exo*-anomeric

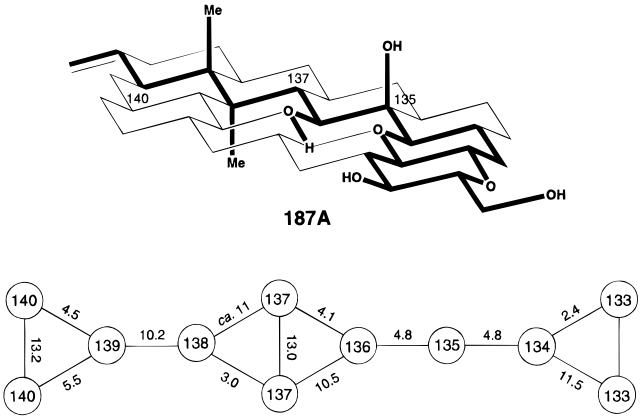

187A

Figure 5. Preferred solution conformation of **187** (top), based on selected vicinal proton coupling constants in Hz (bottom: 500 MHz; 1:1 $C_5D_5N-CD_3OD$).

(58) Li, G.; Still, W. C. *J. Am. Chem. Soc.* **1993**, *115*, 3804−3805 and references cited therein.

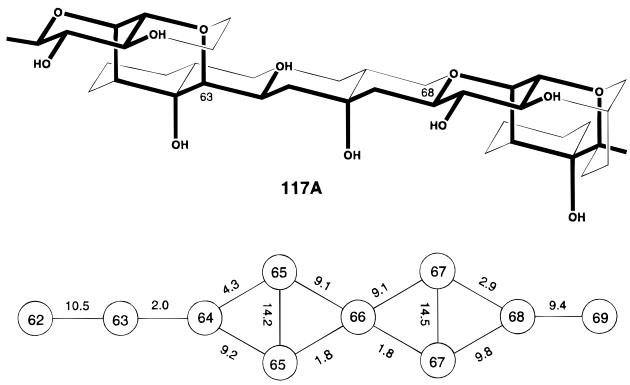

117A

Figure 6. Preferred solution conformation of **117** (top), based on selected vicinal proton coupling constants in Hz (bottom: 500 MHz; 1:1 $C_5D_5N-CD_3OD$).

conformation, which is fully consistent with numerous examples studied in this laboratory.[59] Second, as seen from the conformation drawn on a diamond lattice,[59] the C.135 hydroxyl, C.138 methyl, and C.139 methyl do not cause steric destabilization due to 1,3-diaxial-like interactions,[59,60] whereas the C.136 hydroxyl group has a 1,3-diaxial-like relationship with the C.134 C−O bond. However, it should be noted that 1,3-diaxial-like interactions involving two C−O bonds are much less significant than ones involving one or two C−C bonds. In addition, in this conformation, the C.136 hydroxy group and the ring oxygen on the F′ ring are placed well to form a hydrogen bond, which may provide some stabilization. Third, the backbone of this acyclic portion predominantly adopts an extended conformation. Fourth, as noted above, the NMR characteristics observed for model **187** were virtually superimposable on those of the relevant protons and carbons of the natural product, and the preferred conformation of this portion of MTX should adequately be represented by the preferred conformation of **187**.

Analysis of the vicinal proton coupling constants observed for model **117** (Figure 6) clearly demonstrates that the C.63−C.68 portion of **117** and, consequently, of MTX preferentially adopts a well-defined, extended conformation, **117A**. The L/M- and N/O-rings are dioxa-*cis*-decalins, for which two conformations bearing both rings in a chair form were possible. However, the vicinal coupling constants of the ring protons, for example $J_{62,63} = 10.5$ Hz and $J_{68,69} = 9.4$ Hz, demonstrate the preferred conformation of these ring systems to be the one depicted, in which the C.63 and C.68 substituents are equatorial.

Similarly, the preferred solution conformation of the C.35−C.39 portion of the model **81** and, consequently, of MTX is a well-defined, extended conformation, **81A** (Figure 7). Once again, both *C*-glycosidic bonds, i.e., the C.35−C.36 and C.38−C.39 bonds, preferentially adopt the *exo*-anomeric conformation,[59] and there is no obvious steric destabilization due to 1,3-diaxial-like interactions in this acyclic region. Intriguingly, this preferred conformation makes the backbone of MTX turn in the shape of the letter U, cf. the arrows indicating the direction of the carbon backbone.

The C.1−C.15 portion of **51** and, consequently, of MTX is conformationally less well-defined than the other acyclic portions (Figure 8). Assuming an extended conformation for the carbon backbone of **51** and placing the established relative

(59) (a) Wu, T. C.; Goekjian, P. G.; Kishi, Y. *J. Org. Chem.* **1987**, *52*, 4819−4823. (b) Wei, A.; Haudrechy, A.; Audin, C.; Jun, H.-S.; Haudrechy-Bretel, N.; Kishi, Y. *J. Org. Chem.* **1995**, *60*, 2160−2169 and references cited therein.

(60) The destabilization energy for 1,3-diaxial Me/Me, Me/OH, and OH/OH groups on a cyclohexane ring have been estimated to 3.7, 2.7−1.9, and 1.9 kcal/mol, respectively; see: Corey, E. J.; Feiner, N. F. *J. Org. Chem.* **1980**, *45*, 765−780 and references cited therein.

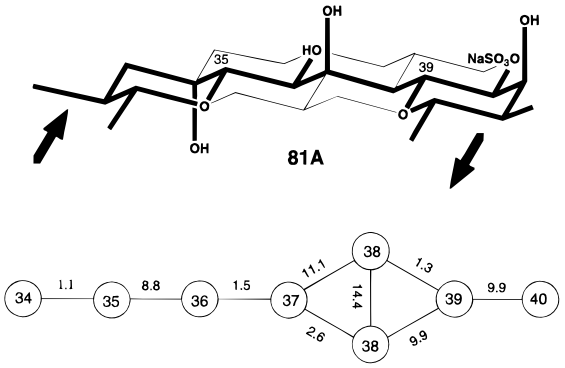

Figure 7. Preferred solution conformation of **81** (top), based on selected vicinal proton coupling constants in Hz (bottom: 500 MHz; 1:1 $C_5D_5N-CD_3OD$).

stereochemistry on this extended backbone provide a clear picture for conformational analysis, cf. the conformer **51A**; the C.7 Me/C.9 OSO_3^- groups and the C.12 Me/C.14 Me groups are in 1,3-diaxial-like relationship and cause severe steric destabilization.[59,60] The vicinal proton coupling constants observed for the C.7−C.9 and C.12−C.14 regions indeed indicate that the carbon backbone of **51** does not adopt preferentially the ideal extended conformation.

With respect to the C.7−C.9 region, there are two conformers, **51B** and **51C**, which are free from the steric destabilization due to the 1,3-diaxial-like interactions, **51B** resulting from rotation of the C.7−C.8 bond of **51A**, and **51C** resulting from rotation of the C.8−C.9 bond of **51A** (Figure 8). The observed vicinal proton coupling constants, $J_{7,8} = 5.7$ Hz and $J_{8,9} = 5.1$ Hz,[61] may suggest the conformational properties of this region to be described primarily by rapid interconversion between these two conformers. Indeed, the NOESY experiments[62] showed clearly the cross peak between the C.6 and C.9 protons, which is obvious in the conformer **51B** but not in the conformer **51C**, as well as between the C.9 and C.7-methyl protons and the C.7 and C.10 protons, which are contrarily obvious in the conformer **51C** but not in the conformer **51B**.

The conformational analysis of the C.12−C.14 region can be treated in a similar manner. The extended conformer **51A** suffers from steric destabilization due to the 1,3-diaxial-like interactions, whereas the conformer **51D** is free from such steric destabilization and the conformer **51E** is less sterically destabilized than the extended conformer **51A**.[59,60] The vicinal proton spin coupling constants, $J_{12,13} = 5.4$ Hz and $J_{13,14} = 6.3$ Hz,[61] may indicate the conformational properties of this region to be described primarily by rapid interconversion between these two conformers, with more weight on **51D**. Once again, the NOESY experiments[61] showed clearly the cross peaks between the C.12 and C.14-methyl protons and the C.11 and C.14 protons, cf. the conformer **51D**, as well as between the C.12 and C.15 protons and the C.14 and C.12-methyl protons, cf. the conformer **51E**. It is interesting to note that the conformation found in the X-ray analysis of **50** (Figure 2) corresponds to the conformer **51D**.

Assembling the preferred solution conformations found for the four acyclic portions allows us to suggest that the approximate global conformation of MTX is represented by the shape of a hook, with the C.35−C.39 portion being the curvature. As pointed out, MTX is conformationally rather rigid, except for the C.7−C.9 and C.12−C.14 portions, which are expected to provide conformational flexibility.

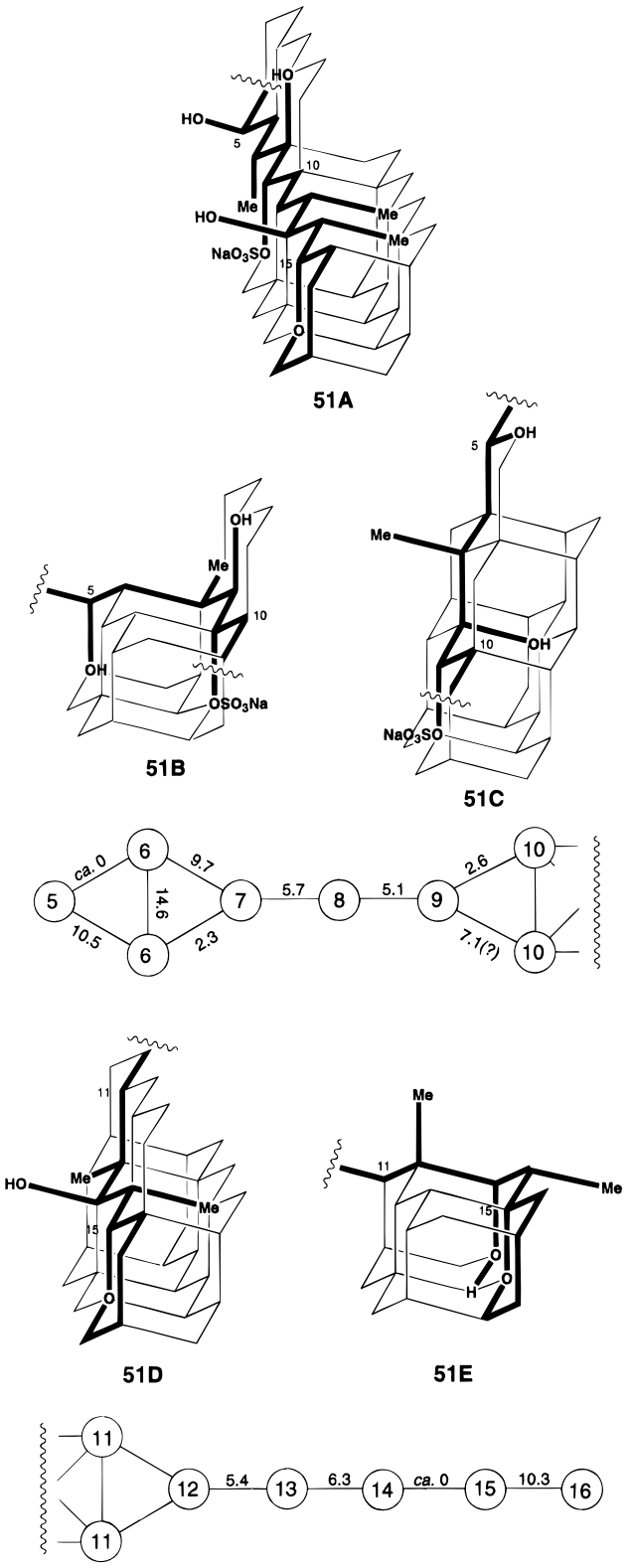

Figure 8. Preferred solution conformation of **51**: **51A**, a hypothetical, extended conformer; **51B**,**C**: two preferred conformers with respect to the C.7−C.9 portion and selected vicinal proton coupling constants in hertz (500 MHz; 1:1 $C_5D_5N-CD_3OD$); **51D**,**E**, two preferred conformers with respect to the C.12−C.14 portion and selected vicinal proton coupling constants in hertz (500 MHz; 1:1 $C_5D_5N-CD_3OD$).

V. Closing Comments

It is remarkable and intriguing that the four small acyclic models **51**, **81**, **117**, and **187**, even much smaller models **9** and

(61) The very similar vicinal proton coupling constants were recorded on the smaller models **9** ($J_{7,8} = 6.1$ Hz and $J_{8,9} = 5.4$ Hz) and **35** ($J_{12,13} = 5.5$ Hz and $J_{13,14} = 6.8$).

(62) These NOESY experiments were conducted on **51**, **viii** (footnote 28), **9**, and **35**. Interestingly, no definitive cross peaks which might be expected for conformer **51A** were detected.

35, beautifully represent the structural characteristics of the corresponding portions of MTX itself. In connection with this, we should point out once again the fact that all eight diastereomers of the left half of the AAL toxin backbone as well as all four diastereomers of the right half exhibited differing and distinct spectroscopic behavior from each other, and this trend was also recognized on all the acyclic portions of MTX. This implies that the structural properties of these substances are inherent to the specific stereochemical arrangement of the small substituents on the carbon backbone, and independent from the rest of the molecules. In other words, each of these diastereomers has the capacity to install a unique structural characteristic through a specific stereochemical arrangement of small substituents on the carbon backbone. Then, it is tempting to suggest the possibility that fatty acids and related classes of compounds may be able to carry specific information and serve as functional materials in addition to structural materials.

VI. Experimental Section

In order to save the journal space, the experimental details, including synthetic procedures and spectroscopic data, are included in the supporting information.

Acknowledgment. Financial support from the National Institutes of Health (NS 12108), the National Science Foundation (CHE 94-08247), and Eisai Pharmaceutical Company is gratefully acknowledged. Dr. A. Marcus Semones in this group is gratefully acknowledged for the X-ray analysis of **50**.

Supporting Information Available: The experimental details, including the synthetic procedures and spectroscopic data (54 pages). See any current masthead page for ordering and Internet access instructions.

Note Added in Proof. (a) On exchanging manuscripts with the Tachibana/Yasumoto group (June 27, 1996), we learned that they have reached the same conclusion by a different approach.

(b) According to a fax letter from Dr. Murata (July 1, 1996), the C.3 carbon chemical shift was incorrectly reported (see ref 26); the correct chemical shift is 136.0 ppm, which matches perfectly with the values observed for the remote diastereomers **51** (135.8 ppm) and **52** (135.8 ppm) and also for two additional models **vii** (136.0 ppm) and **viii** (135.9 ppm) mentioned in ref 27.

(c) We have recently completed the synthesis and NMR studies of the models **xi** and **xii**, representing the two possibilities for the stereochemistry of the V/W-ring juncture (see ref 53). As seen from the charts below ($\Delta\delta$(ppm) = $\delta_{MTX} - \delta_{SyntheticModel}$ in ^{1}H (500 MHz) and ^{13}C (125 MHz) chemical shifts in 1:1 $C_5D_5N-CD_3OD$ between MTX and **xi** and **xii**, respectively), it is now evident that the original assignment, cf. **ix** in ref 53, of the ring juncture is correct: Oinuma, H.; Cook, L. R.; Kishi, Y. Unpublished work.

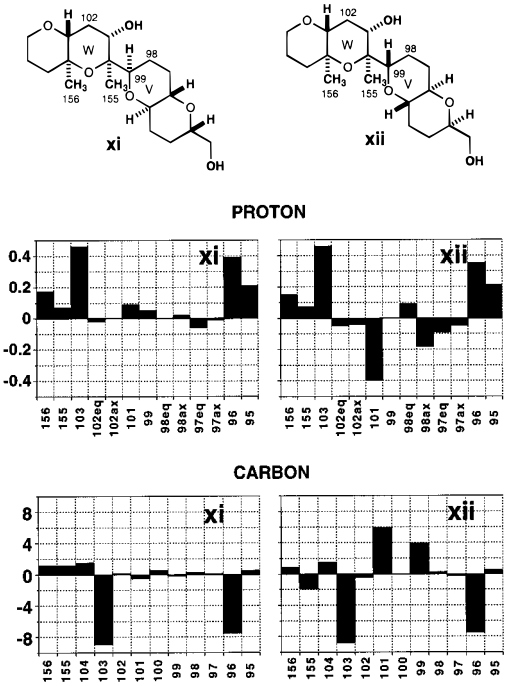

(d) We learned that Tachibana and co-workers have recently concluded the absolute configuration of MTX to be represented by **1C** via (1) degradation of MTX ($NaIO_4$ oxidation, followed by $NaBH_4$ reduction) to the C.136−C1.42 primary alcohol and (2) chiral gas chromatographic analysis of the resultant primary alcohol. We have also developed a method to determine its absolute configuration, which involves (1) degradation of MTX to the C.136−C.142 primary alcohol via the known procedure,[6c] (2) its esterification with a β-naphthyl analog of Mosher acid, and (3) HPLC analysis. The naphthyl analog of Mosher acid was used for improvement of the sensitivity of detection; it allowed an analysis of the absolute configuration of MTX with much less than 0.01 mg. The absolute configuration of MTX from two different sources, Wako Chemicals USA (Catalog No. 131-10731, Lot YLE9504) and Calbiochem-Novabiochem (Catalog No. 442620, Lot B 11288), has recently been examined by this method: Kim, H.; Kishi, Y. Unpublished results.

JA961230+

(63) Related to this, we should mention a recent example from this laboratory, which demonstrated that the binding affinity of the H-type II human blood group determinant toward the lectin I was strongly affected by changes in their preferred solution conformation at the ground state (Wei, A.; Boy, K. M.; Kishi, Y. *J. Am. Chem. Soc*. **1995**, *117*, 9432−9436).

(64) Evans, D. A.; Fu, G. C.; Hoveyda, A. H. *J. Am. Chem. Soc*. **1988**, *110*, 6917−6918; **1992**, *114*, 6671−6679.

(65) Compound *((E)*-4-(*tert*-butyldimethylsiloxy)-2-buten-2-yl)lithium was prepared by lithiation (*t*-BuLi, THF, −78 °C, 30 min) of *(E)*-4-(*tert*-butyldimethylsiloxy)-2-buten-2-yl bromide.[25]

(66) (4-(1-Ethoxyethoxy)-3,3-dimethylbutyl)lithium was prepared by lithiation (*t*-BuLi, THF, −78 °C, 30 min) of 4-(1-ethoxyethoxy)-3,3-dimethylbutyl bromide, which was in turn prepared from 3,3-dimethyloxetane in four steps: (1) vinyllithium, $BF_3{\cdot}OEt_2$, −78 °C; (2) ethyl vinyl ether, *p*-TsOH; (3) O_3, MeOH then $NaBH_4$; (4) Ph_3P, imidazole, Br_2.

(67) Bocker, T.; Lindhorst, T. K.; Thiem, J.; Vill, V. *Carbohydr. Res.* **1992**, *230*, 245−256.

(68) HF·pyr was prepared by mixing 30.0 g of aqueous HF (49%) and 14.9 mL of pyridine.

(69) (a) Araki, S.; Ito, H.; Butsugan, Y. *J. Org. Chem.* **1988**, *53*, 1831−1833. (b) Kim, E.; Gordon, D. M.; Schmid, W.; Whitesides, G. M. *J. Org. Chem*. **1993**, *58*, 5500−5507 and references cited therein.

(70) Compound 4-(*tert*-butyldimethylsiloxy)-1-buten-2-yl iodide was prepared from 3-butyn-1-ol in three steps: (1) *n*-Bu_3SnH, CuCN, *n*-BuLi; (2) TBSCl, imidazole, DMF; (3) I_2.

(71) (a) Mahoney, W. S.; Brestensky, D. M.; Stryker, J. M. *J. Am. Chem. Soc*. **1988**, *110*, 291−293. (b) Koenig, T. M.; Daeuble, J. F.; Brestensky, D. M.; Stryker, J. M. *Tetrahedron Lett.* **1990**, *31*, 3237−3240 and references cited therein.

(72) (a) Seyferth, D.; Simmons, H. D., Jr.; Singh, G. *J. Organomet. Chem.* **1965**, *3*, 337−339. (b) Seyferth, D.; Heeren, J. K.; Singh, G.; Grim, S. O.; Hughes, W. B. *J. Organomet. Chem.* **1966**, *5*, 267−274.

(73) Williams, D. R.; White, F. H. *J. Org. Chem.* **1987**, *52*, 5067−5079.

(74) (a) Nozaki, K.; Oshima, K.; Utimoto, K. *J. Am. Chem. Soc.* **1987**, *109*, 2547−2549. (b) Nozaki, K.; Oshima, K.; Utimoto, K. *Tetrahedron* **1989**, *45*, 923−933.

(75) Hofmeister, H.; Laurent, H.; Schulze, P.-E.; Wiechert, R. *Tetrahedron* **1986**, *42*, 3575−3578.

(76) Mahler, H.; Braun, M. *Tetrahedron Lett.* **1987**, *28*, 5145−5148.

(77) Grieco, P. A.; Miyashita, M. *Tetrahedron Lett.* **1974**, 1869−1871.

(78) Mori, K.; Ueda, H. *Tetrahedron* **1982**, *38*, 1227−1233.

(79) Yamamoto, Y.; Nishii, S.; Ibuka, T. *J. Chem. Soc., Chem. Commun.* **1987**, 1572−1573.